Sedimentology (1996) **43**, 295–322

Facies and cyclicity of the Late Permian Bainmedart Coal Measures in the Northern Prince Charles Mountains, MacRobertson Land, Antarctica

CHRISTOPHER R. FIELDING* and JOHN A. WEBB†
**Department of Earth Sciences, University of Queensland, St Lucia, Qld 4072, Australia (E-mail: chrisf@earthsciences.uq.edu.au)*
†School of Earth Sciences, LaTrobe University, Bundoora, Vic. 3083, Australia (E-mail: geojaw@lure.latrobe.edu.au)

ABSTRACT

The Late Permian Bainmedart Coal Measures form part of the Permo-Triassic Amery Group, which crops out in the Beaver Lake area of the Northern Prince Charles Mountains, MacRobertson Land, Antarctica. The exposed strata are believed to have formed in graben or half-graben sub-basins on the western edge of the Lambert Graben, a major failed rift system. Sedimentological analysis has revealed that these rocks formed in alluvial environments in which swiftly flowing rivers of low sinuosity (represented by Facies A1 and A2) flowed northward down the axis of the basin, and were associated with waterlogged floodbasin and peat-forming wetlands (Facies B1–B4). A third Facies Association (comprising Facies C1–C3), interpreted as the deposits of lake floor and delta environments, is exclusively developed within a distinctive, fine-grained interval here named the Dragon's Teeth Member. The proportion of Association B facies within the succession increases markedly above the level of the Dragon's Teeth Member (at about 300 m above the base of the formation).

Flat, low-angle and undulatory bedding structures preserved within channel deposits are suggestive of sediment deposition in flow conditions which were often critical or supercritical. Presence of massive and chaotic intervals of sandstone further implies some deposition from high-concentration aqueous flows. Alluvial channel bodies show evidence of incision into underlying substrates, both during initiation and at later stages in channel belt construction. The lack of interfingering between channel deposits and coals suggests that thick peats formed only in areas and at times of minimal clastic sediment supply.

Analysis of well-developed cyclicity within the coal measures suggests that the dominant control on sequence architecture was climatic, related to precessional Milankovitch fluctuations of *c.* 19-kyr periodicity. Cycles began abruptly with the deposition of coarse-grained material in high-energy alluvial channels, which contracted with time in response to changes in water supply (rainfall). Upper parts of cycles are dominated by finer-grained sediments and then coal, indicative of progressively reduced coarse sediment input. Tectonic processes overprinted this pattern at least once during the period of sediment accumulation, to form the Dragon's Teeth Member.

INTRODUCTION

Descriptions of alluvial coal-bearing systems are common in the geological literature. Papers based on detailed examination of large-scale exposures, which contribute to the understanding of sequence architecture, are nonetheless more limited. In the analysis of coal-bearing

successions, the opportunity exists to re-create depositional history in more detail than with other nonmarine successions because of the large number of correlatable horizons available. In addition to improving our understanding of coal depositional environments, the analysis of alluvial coal measures will shed new light on controls on nonmarine basin evolution.

This paper describes and interprets the deposits of a coal-bearing, high-energy alluvial system from East Antarctica. The Late Permian Bainmedart Coal Measures form part of the fill of a narrow, corridor-like basin which is interpreted as the remnant of a continental graben or half-graben. The examination of both lateral sediment body geometry and vertical sequence aspects allows considerable insights into the controls on sediment deposition and accumulation. We conclude that the dominant control on sediment body architecture is climatic and that, by analogy, similar basin fills elsewhere may also preserve a record of climatic fluctuation.

REGIONAL GEOLOGY AND STRATIGRAPHY OF THE AMERY GROUP

The only known surface exposure of Palaeozoic sedimentary rocks in East Antarctica lies in the Beaver Lake area of the northern Prince Charles Mountains (Fig. 1). The Permo-Triassic Amery Group (Crohn, 1959; Mond, 1972; Webb & Fielding, 1993a) comprises more than 2000 m of clastic sedimentary rocks interbedded in places with coal seams. These rocks crop out in spectacular cliffs around two ice-covered water bodies, Beaver Lake (in reality a tidal inlet) and the smaller Radok Lake (Fig. 1). Geophysical data (Fedorov *et al.*, 1982) suggest that the Amery Group crops out on the western margin of the north–south elongate Lambert Graben, a major failed continental rift system with a multiphase history. The Lambert Graben is almost entirely covered by the Lambert Glacier, the largest valley glacier in the modern world, and outcrop data are scarce. The Beaver Lake 'graben' is interpreted as a sub-basin of the main Lambert Graben, as it has a similar trend and evidence of faulted boundaries (Fig. 1).

The Amery Group was divided into three formations by Mond (1972); his basic subdivision has been retained to the present although some stratigraphic revisions have been proposed

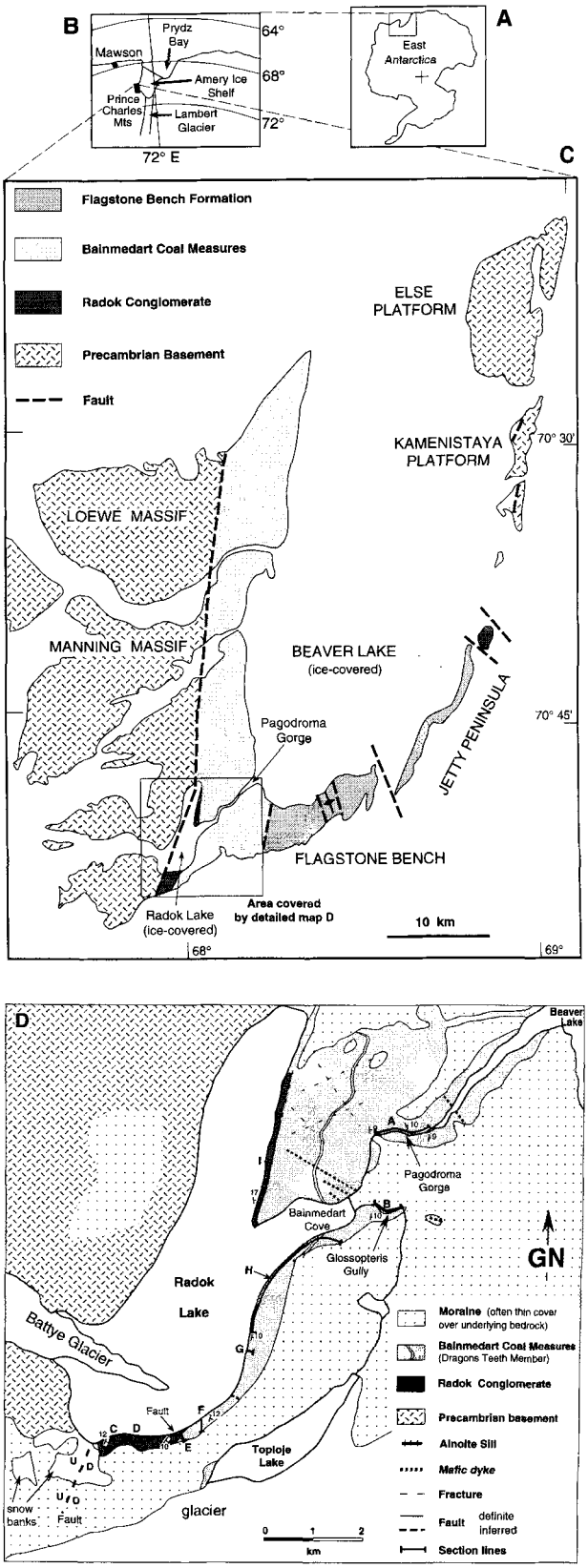

Fig. 1. Maps showing the study area within the northern Prince Charles Mountains of East Antarctica, and location of logged sections.

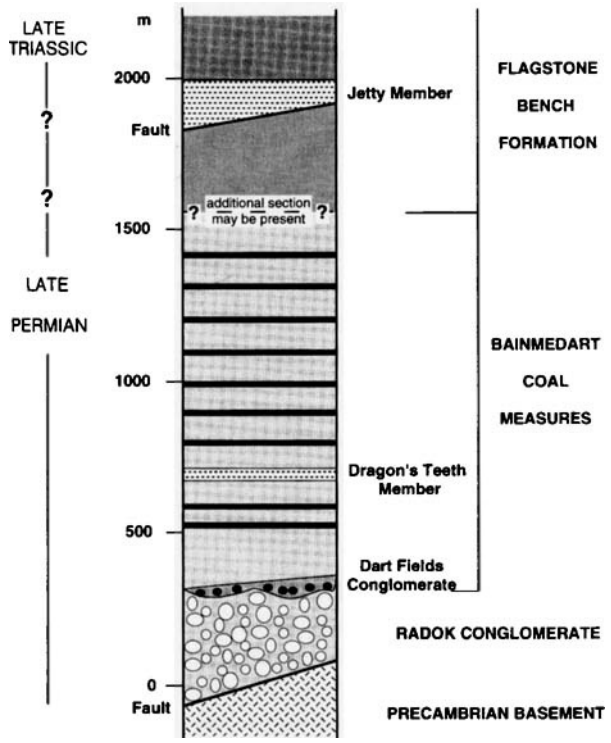

Fig. 2. Stratigraphic column for the Permo-Triassic Amery Group in the Beaver Lake area.

(Ravich *et al.*, 1977; McKelvey & Stephenson, 1990; Webb & Fielding, 1993a,b; Fig. 2). The lowermost Radok Conglomerate comprises at least 400 m of interbedded conglomerates, sandstones, mudrocks and thin coals, and is interpreted by Fielding & Webb (1995) as a piedmont alluvial apron deposit associated with extensional fault activity along Permian rift margins. The overlying Late Permian Bainmedart Coal Measures, the subject of this paper, consist of about 1100 m of sandstone-dominated strata with coal seams up to 8 m in thickness. This unit is in turn overlain by the similarly sandstone-dominated, Late Permian to Late Triassic Flagstone Bench Formation, which is devoid of coal and contains reddened mudrocks (Webb & Fielding, 1993a). This unit was deposited in mainly axially (northward)-draining rivers (Webb & Fielding, 1993a). Recent mapping (S. McLoughlin & A. N. Drinnan, unpubl. obs.) has shown that additional units lie between the Bainmedart Coal Measures and Flagstone Bench Formation as here defined. The base and top of the Amery Group are unexposed, but a minimum total thickness of 3000 m has been estimated from the Beaver Lake outcrop (S. McLoughlin & A. N. Drinnan, unpubl. obs.).

Fig. 3. View of cliffs along the north-eastern side of Radok Lake (looking south-east), showing the contact between dark-coloured, heterolithic Radok Conglomerate and overlying Bainmedart Coal Measures. Total height of exposure 85–90 m. Note large-scale channel forms in basal Coal Measures sandstones near the right-hand (south) end of cliffs.

BAINMEDART COAL MEASURES – GENERAL CHARACTERISTICS

The base of the Bainmedart Coal Measures (BCM) is marked by a prominent lithological, compositional and colour change in outcrop (Fig. 3). The light-coloured, quartzofeldspathic sandstones of the basal BCM contrast markedly with the matrix-rich, brown- and olive-coloured rocks of the uppermost Radok Conglomerate. The contact is mantled by a discontinuous but laterally extensive, pebble to boulder conglomerate bed, named formally by McKelvey & Stephenson (1990) as the Dart Fields Conglomerate Member (of the BCM). The boundary is disconformable to locally unconformable (Fielding & Webb, 1995).

The lowermost 300 m of the BCM are composed essentially of thick, amalgamated sheet sandstone bodies, separated by thin (<1 m) mudrock and/or coal beds (Fig. 4). Above this interval lies a distinctive, brown-weathering, fine-grained unit some 20 m thick, which warrants separation as a Member (here termed the Dragon's Teeth Member, after the nearby Dragon's Teeth Cliffs: Appendix 1). Above this useful marker horizon, the BCM become less sandstone-dominated, and both the gross percentage and individual bed thicknesses of coal seams increase markedly. Nearly all coals greater than 0·4 m thick are located above this horizon. The top of the unit is obscured by a deep snow-covered gully and moraine on Flagstone Bench, but McLoughlin & Drinnan (in press) suggest a faulted contact with the overlying Flagstone Bench Formation (Fig. 1).

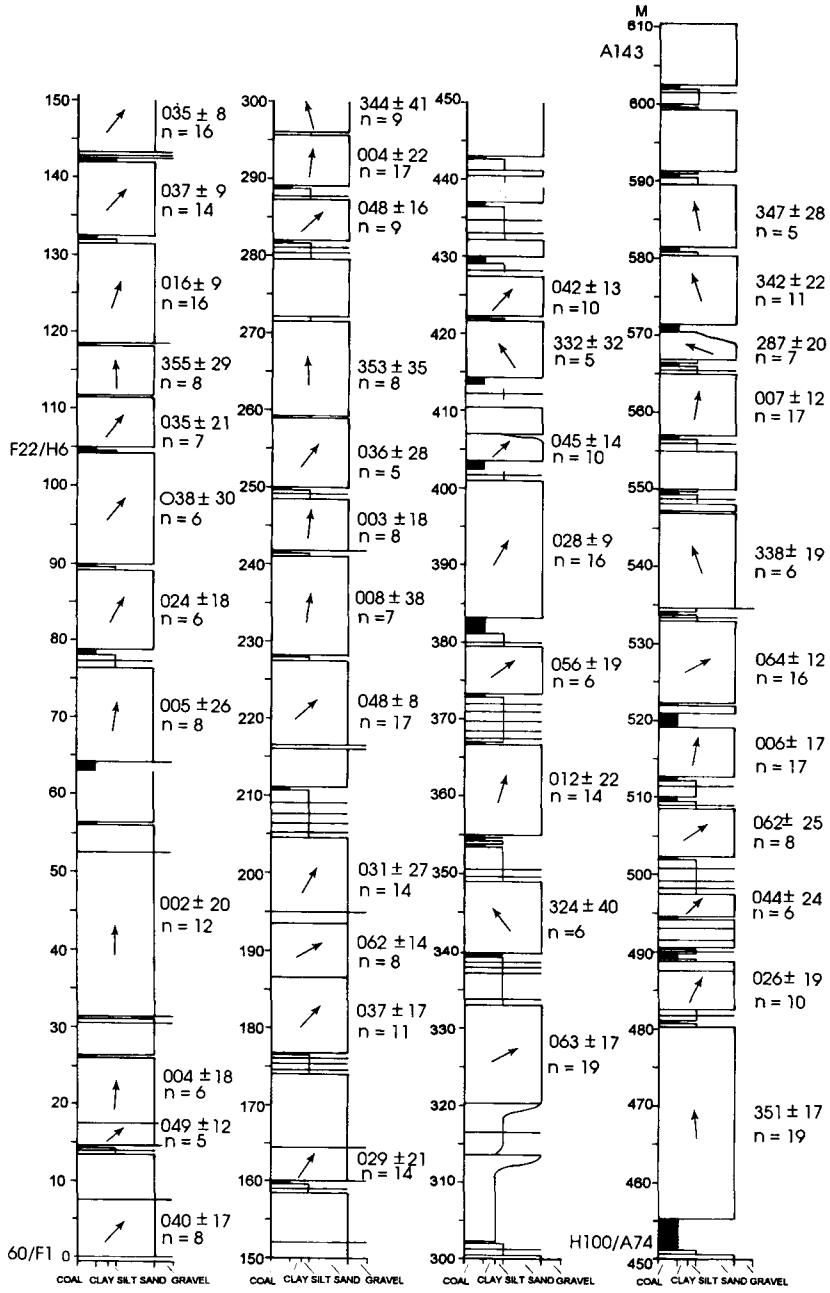

Fig. 4. Generalized graphic log showing a composite section through the lower 600 m of the Bainmedart Coal Measures (see Figs 1D & 5 for details of section locations and equivalence). Palaeocurrent mean directions for individual channel sandstone bodies (Facies A1) illustrate the low variance in sediment dispersal direction throughout the accumulation of this interval.

Sandstones within the BCM are typically yellowish grey (5Y7/2–5Y8/1) in colour, whereas mudrocks are generally light to dark grey (N3–N7). The sandstones are medium- to coarse-grained subarkoses to sublitharenites (Folk *et al.*, 1970); a few are feldspathic wackes. Framework grains are composed of monocrystalline quartz (*c.* 46%), polycrystalline quartz (*c.* 4%), feldspars (*c.* 15%; predominantly microcline and orthoclase, often perthitic, with some plagioclase), lithic grains (*c.* 10%; mainly metamorphic rock fragments) and minor amounts of heavy and opaque minerals. Some sandstones also contain up to a few per cent muscovite and biotite. Organic matter (carbonized plant material) is common in some samples, concentrated in laminae together with micas.

Matrix is present in all sandstones, in amounts ranging from trace to 50%. In many samples it is evidently of primary depositional origin, consisting of very fine-grained quartz and plastically deformed clay grains, but in other samples it is

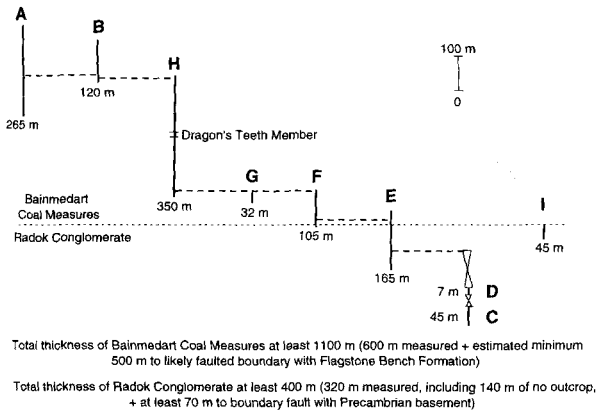

Fig. 5. Diagram showing stratigraphic equivalence between measured sections, based on direct physical correlation.

predominantly diagenetic kaolinite. Thin, syntaxial quartz overgrowths surround many quartz grains, particularly in areas lacking substantial matrix. Siderite often occurs as an alteration product of biotite and as replacement of some carbonized plant material. Ferroan calcite occurs locally as a pore-filling cement and as a replacement of some minerals, notably orthoclase. In one sample, a fracture perpendicular to the bedding is filled with dark matter largely replaced by an iron sulphide (probably pyrite). It is possible that heavy oil originally filled the fracture.

The BCM contain only nonmarine plant fossils (White, 1973). Macrofossils recovered to date include *Glossopteris* leaves, *Paracalamites* stems, *Vertebraria* roots and rootlets, and petrified wood and peat at one horizon (base of the Dragon's Teeth Member). Palynological studies (Playford, 1990) have not identified any marine influence. The flora suggests that the unit accumulated under humid, cool-temperate climatic conditions.

The apparently fluviatile nature of the succession, coupled with the complete lack of marine fossils, together argue persuasively for an alluvial environment of deposition. The lithofacies of the Bainmedart Coal Measures are described and interpreted in detail in the following passages. From this facies analysis, an understanding of the depositional environment and temporal evolution of the BCM system is developed, and possible controls on its formation explored. This analysis is based on field data collected as a series of composite vertical sections and lateral profiles. The location of vertical sections is shown on Fig. 1, and correlations between sections are given in Fig. 5.

FACIES ANALYSIS

A total of nine lithofacies have been recognized in the BCM, of which three are confined to the Dragon's Teeth Member. Facies have been divided into three facies associations, reflecting the major component depositional systems of the BCM; (A) Major Alluvial Channel, (B) Floodbasin and (C) Permanent Lake. Essential details of these facies and their interpreted context are given in Table 1, and examples of vertical and lateral facies associations in Fig. 6.

Association A – Major Alluvial Channel

Facies A1 – active channel fills

Description. Facies A1 comprises up to 25-m-thick, sheet-like, erosive-based bodies of sandstone, internally dominated by trough cross-bedding (Table 1). Bases of sandstone bodies are invariably sharp, undulating contacts displaying up to 3 m of relief (Fig. 7a,b). Basal contacts are commonly lined by a layer of well-rounded quartzite and vein quartz clasts up to 44 cm in diameter, and gutter casts occur in some instances. Siltstone clasts up to 2 m long and flattened, coaly compressions of tree trunks up to 0·5 m wide are also abundant in the basal parts of sandstone bodies, which are in many cases chaotically bedded. Some sandstone bodies fine upwards, but most fluctuate irregularly in grain size or show no major vertical grain-size changes. Upper contacts are variable in character, some being sharp whereas others are gradational or interbedded (Fig. 7). Where exposed, lateral margins to sandstone bodies are wedge-shaped pinchouts, incised by up to 8 m into previously deposited sediments (Fig. 7c).

Most sandstone bodies are multistorey, composed of an overlapping arrangement of sheet-like subunits. Each storey is bounded by flat-lying but undulating erosion surfaces (Figs 3 and 7a–c). Channellized scours are visible in some bodies (e.g. Fig. 7a): these truncate the flat-lying bounding surfaces, are roughly symmetrical with a concentric fill, and range in cross-sectional dimensions from broad and shallow (1 × 20 m) to deeply incised (10 × 40 m). Each storey is internally dominated by trough cross-bedding in sets up to 1·5 m thick (mostly <0·5 m), with variable development of convolute bedding and lesser abundances of other current-generated sedimentary structures. Trough cross-beds are gently curved in both plan and cross-sectional view, and

Table 1. Characteristics of Bainmedart Coal Measures lithofacies.

Association/facies	Interpretation	Lithology	Sedimentary structures	Biota	Geometrical data
A – Major Alluvial Channel					
A1	Active fill of major alluvial channels	Medium- to very coarse-grained sandstone in erosively based bodies <25 m thick, some upward fining, sharply or gradationally topped	Gently curved trough cross-bedding in sets <1·5 m, undulatory (?standing wave) bedding, flat and low-angle lamination, convolute bedding, less abundant ripple cross-lamination	Flattened compressions of tree trunks, rare meandering trails	North–south elongate sheets of uncertain width, typically incised lateral margins, tabular cross-sectional geometry. Mean palaeoflow to 025° (n=792)
A2	Abandonment fill of major alluvial channels	Interbedded very fine- to medium-grained sandstone and siltstone, fining-upward units <5 m thick	Ripple cross-lamination and small-scale trough cross-bedding, load casting, interlamination structures	Plant debris, *in situ* rootlets, indeterminate bioturbation	Irregular, ?elongate external geometry, may contain dipping major stratal surfaces (lateral accretion deposits) and channel forms. Palaeoflow variable
B – Floodbasin					
B1	Proximal overbank	Sharply bounded sandstone units <1·5 m thick interbedded with thin-bedded sandstone/siltstone	Trough cross-bedding, ripple and climbing ripple cross-lamination, flat and low-angle lamination, convolute bedding, load casting	Plant debris, *in situ* rootlets and upright tree stumps, rare simple bioturbation	Overall extensive sheet geometry, individual sandstone units tabular, continuous over at least 200 m. Palaeoflow variable
B2	Overbank	Thin-bedded siltstone and sandstone, with rare sandstone beds <1·0 m	Trough cross-bedding, ripple cross-lamination, interlamination structures, soft sediment deformation structures, rare wave ripples	Plant debris, *in situ* rootlets and upright tree stumps, rare simple bioturbation	Overall extensive sheet geometry, individual beds variable, some depositional dips and small channel forms
B3	Distal floodbasin	Thinly laminated siltstone and claystone, minor thin sandstones	Interlamination structures	As above	Overall sheet geometry
B4	Mire	Coal and carbonaceous shale, very rare clastic partings	Compositional banding/bedding	Plant debris	Simple sheet geometry, no splits noted
C – Permanent Lake					
C1	Lake floor	Fissile, carbonaceous claystone (shale), up to 9 m thick with small, discoid carbonate concretions	Flat bedding	Leaves and fine plant debris, ?bivalve shell	Extensive sheet geometry

Table 1. *Continued.* Characteristics of Bainmedart Coal Measures lithofacies.

Association/facies	Interpretation	Lithology	Sedimentary structures	Biota	Geometrical data
C2	Distal lake delta	Thin-bedded siltstone and fine-grained sandstone, up to 5 m thick, generally coarsening-upward	Ripple cross-lamination, interlamination structures	Minor fine plant debris	Uncertain, but irregular
C3	Proximal lake delta	Mainly medium-grained sandstone, beds <0·4 m thick, with minor interbedded siltstone	Undulatory and low-angle lamination, small-scale trough cross-bedding, ripple and climbing ripple cross-lamination, interlamination structures	None noted	Uncertain, but irregular

are almost planar in some cases. Cosets of cross-strata occur in places, but more commonly cross-beds are arranged in a complex cross-cutting mosaic. The thickness of cross-sets commonly decreases upward through individual sandstone bodies. An unusual style of 'humpback' cross-bedding was observed in a few instances, in which topset, foreset and bottomset bedding is preserved together with the external shape of the formative dune (Fig. 7d).

Interbedded with cross-bedded units are intervals dominated by flat lamination, and low-angle lamination which in some cases may be regarded as erosionally truncated cross-bedding but in others displays extensive bottomset preservation and/or a convex-upward cross-sectional geometry. Convex-up bedding structures in some respects resemble low-amplitude forms of hummocky cross-stratification, but differ in not preserving internal truncation surfaces. Some 0·2–0·4-m-thick beds show complete, convex-up, virtually symmetrical bedforms with a wavelength of 1·5–2·0 m, in which internal laminae thicken towards the bedform crest.

Separating the medium- to coarse-grained sandstones described above are lesser intervals of mainly fine-grained, ripple cross-laminated sandstone. Where preserved as form sets, ripples display a straight to sinuous-crested plan morphology. Coaly and silty laminae are common within these lithologies. Thin siltstone partings, where preserved, are of limited lateral extent and typically terminated by erosion at the base of an overlying sandstone.

Facies A1 sandstones are variably affected by soft-sediment deformation, mainly in the form of convolute bedding. This structure is particularly well developed at the tops of storeys, and is invariably found in cross-bedded sandstone. The vertical extent of convolute bedding at any horizon varies laterally, and no deformed unit can be traced over more than a few tens of metres. Oversteepening of cross-strata is also developed in some bodies.

Interpretation. The erosively based, channellized form of Facies A1 sandstone bodies argues persuasively for a channel origin. The sheet-like external and internal (storey) geometry, lack of any evidence of systematic lateral accretion (continuous epsilon cross-strata), and the low dispersion of palaeocurrent data both overall and within individual bodies (Figs 4 and 8) all point towards sediment accumulation in low-sinuosity, braided rivers (cf. Bridge, 1985). The width distribution of

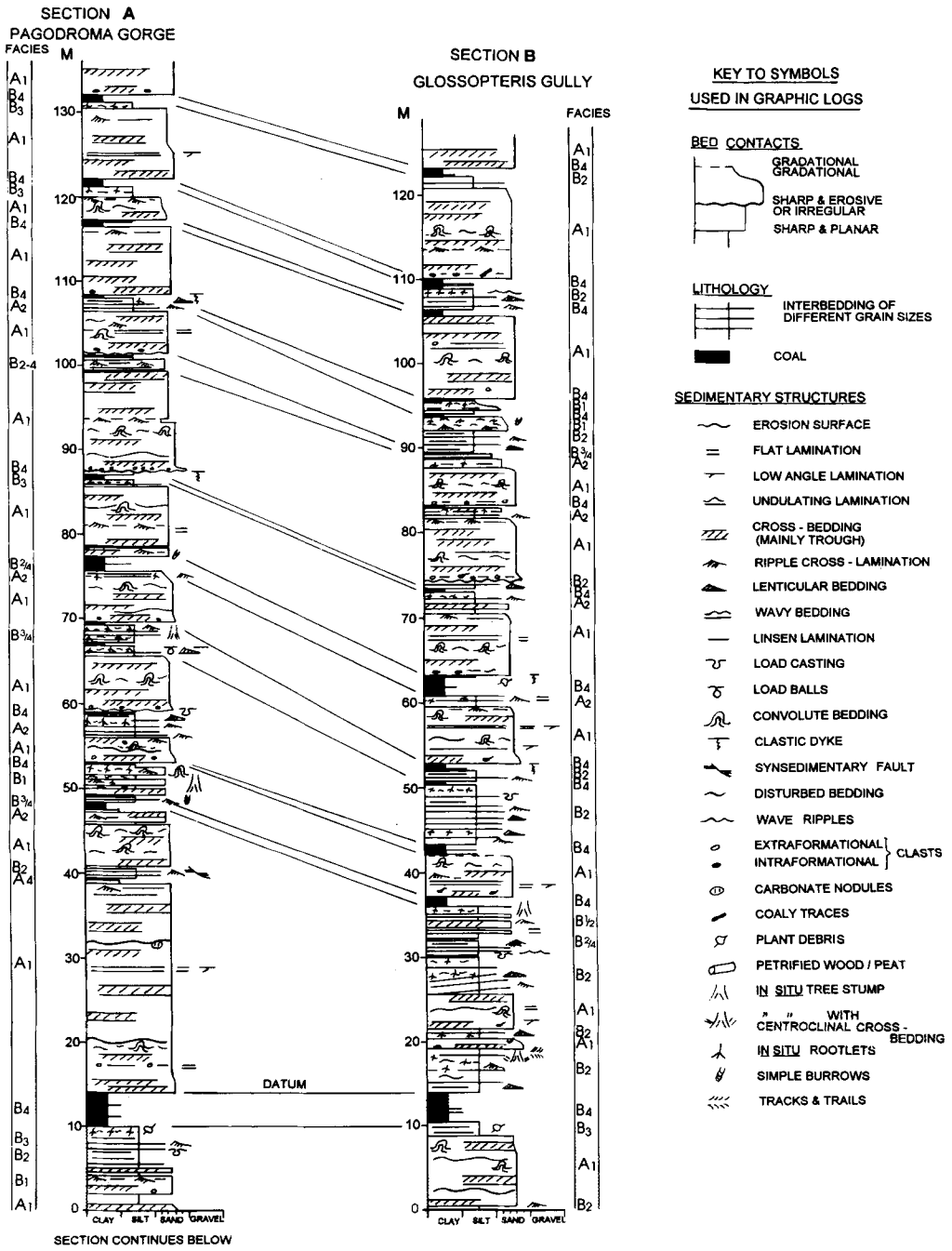

Fig. 6. Graphic logs of measured sections A (Pagodroma Gorge) and B (Glossopteris Gully), illustrating vertical and lateral lithofacies relationships, and key to symbols used in graphic logs. Sections A and B are *c.* 1600 m apart.

Fig. 7. Views of channel sandstones (Facies A1) and associated facies. (a) Section A (Pagodroma Gorge), showing the interval 40–90 m on Fig. 6. Note the abundance of undulating major bedding surfaces which are associated with convolute bedding and other soft-sediment deformation, and the deep, composite channel form (arrowed) towards the right-hand (east) end of the cliff line. Cliff section is perpendicular to palaeoflow. (b) Section A, showing strata below 4 m coal at 10 m in Fig. 6. Note undulatory form of major bedding surfaces (arrowed) in the thick sandstone body in the centre of the view, and a lateral pinchout of a channel sandstone into overbank facies (B2) in the underlying unit (arrowed). Cliff section is perpendicular to palaeoflow; *c.* 45 m of section exposed. (c) Section A, uppermost part (see Fig. 6). Note internal architecture of channel sandstone bodies, and the incised lateral margin of one body towards the left-hand (south-west) end of cliffs (*c.* 45 m of section exposed). (d) Close-up of 'humpback' dune bedform, showing preservation of topset, foreset and bottomset bedding, interpreted as arising from flow conditions transitional between stability fields of dune and plane bed. Hammer 0·25 m long. Section A, at *c.* 20 m in Fig. 6.

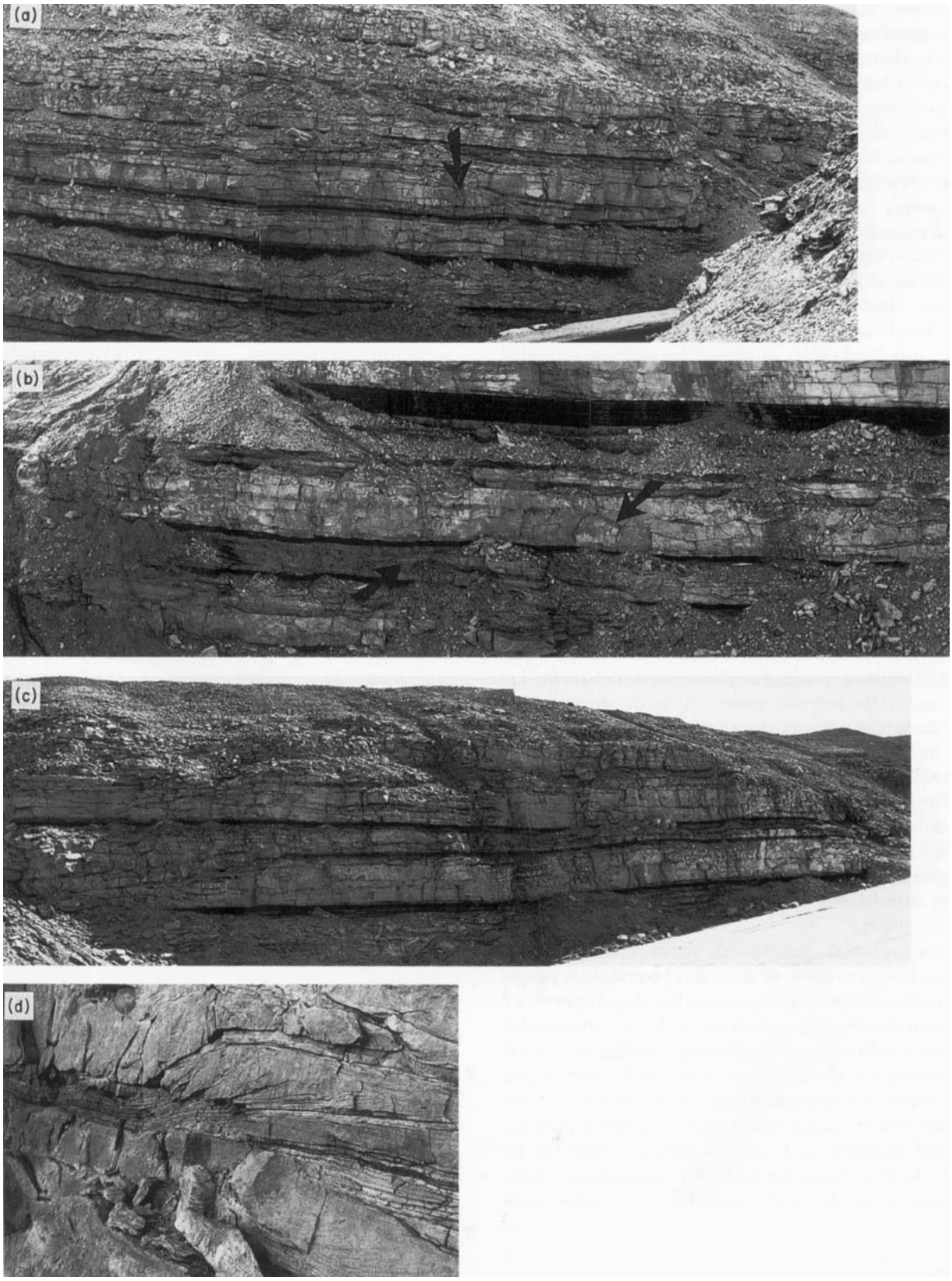
(a)
(b)
(c)
(d)

channels remains unknown, but the internal architecture of Facies A1 suggests that sediments accumulated by switching of active channels across a broad channel belt (see below). Observations from incised channel belt margins and internal channel scours (e.g. Fig. 7a,c) suggest that active channels ranged up to 10 m deep, but were typically 6–8 m. This is supported by a frequency distribution plot of sandstone body thickness (Fig. 9) which shows peaks at 6–8 m and 12–14 m.

Facies A1 is interpreted as the deposits of major, low-sinuosity alluvial channels. The nature of sand accumulation within these channels may be further analysed by reference to the preserved sedimentary structures. The dominance of complexly arranged cross-bedding may be interpreted to record sand deposition on low-relief, slightly sinuous-crested dunes and in associated channel floor scours. Larger-scale cross-bedding is interpreted to reflect the coexistence of up to 1·5-m-high, essentially straight-crested dunes; palaeocurrent relationships suggest that representatives of both downstream- and across-stream-migrating bedforms are preserved. Rarely, compound bedform remnants were noted, consisting of cosets of small-scale cross-bedding replaced down-palaeocurrent by a single, large-scale cross-set with descending intrasets (cf. Haszeldine, 1983). Ripple cross-laminated intervals may be interpreted as remnants of low-stage deposits, and the rare fine-grained partings as largely eroded remnants of slack-water channel or interchannel island deposits (cf. Reinfelds & Nanson, 1993). The geometry of preserved current ripples suggests that equilibrium conditions were rarely achieved (cf. Baas *et al.*, 1993).

The unusual nature of some cross-bedding structures is worthy of further comment. A range of variation in the cross-sectional geometry of cross-strata was noted, from 'normal' avalanche foresets through 'humpback' bedforms with sigmoidal foresets (Fig. 7d) and low-angle, bottomset-dominated forms to undulatory bedding which preserves convex-upward lamina sets. The sigmoidal cross-bedding is similar in style to the 'humpback dunes' produced experimentally by Saunderson & Lockett (1983), and

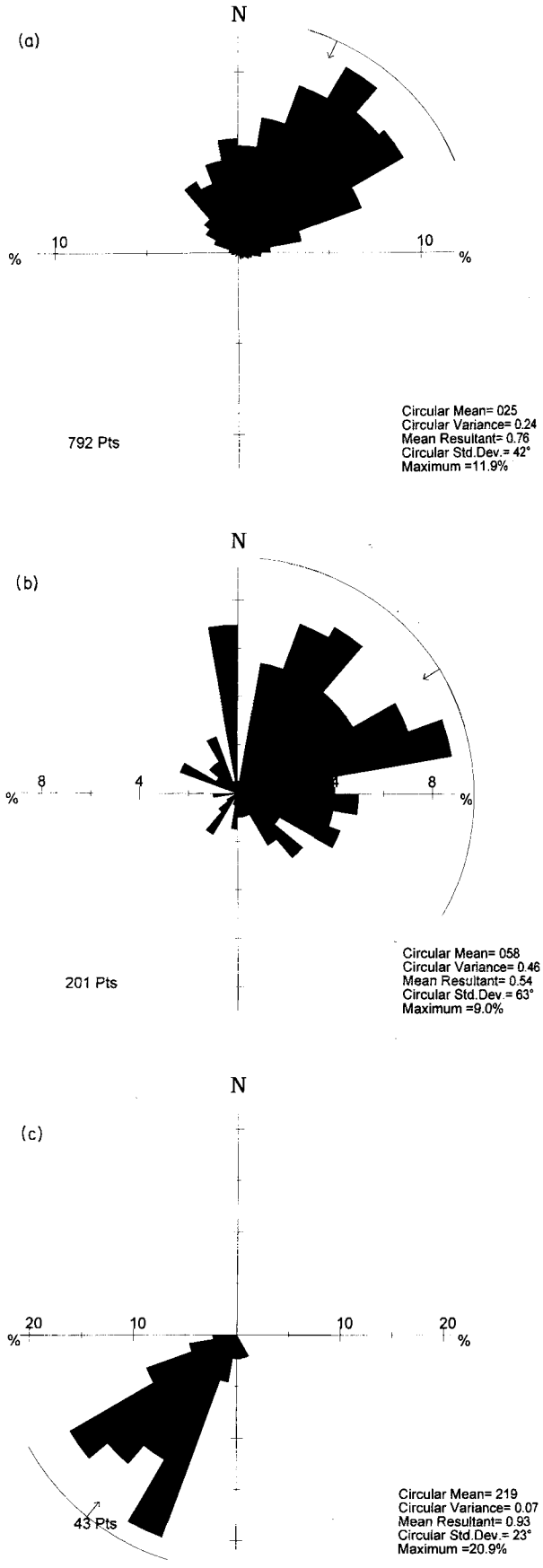

Fig. 8. Rose diagrams summarizing palaeocurrent data collected from sandstones of (a) Facies A1, (b) Facies Association B, and (c) Facies Association C (Dragon's Teeth Member).

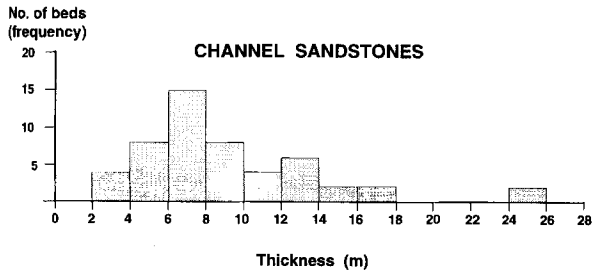

Fig. 9. Distribution plot of Facies A1 sandstone body thickness. Note modes at 6–8 m and 12–14 m, which are interpreted as indicative of formative channel depths typically in the range 6–8 m.

to cross-bedding from ancient sequences described by Roe (1987), Collinson & Thompson (1989; their fig. 6.35) and Roe & Hermansen (1993), in each case ascribed to transitional dune-to-plane bed phase flow conditions. In such near-critical conditions, dunes become progressively flattened out at higher values of the Froude number (Harms *et al.*, 1975; Saunderson & Lockett, 1983). The low-angle, bottomset-dominated cross-bedding is considered a logical extension of the previous bedding style, formed in transitional upper-flow-regime (critical) conditions similar to those described by Langford & Bracken (1987). Flat lamination with attendant parting lineation is interpreted to represent plane bed conditions, and the undulating, convex-up bedding as recording flow transitional to (and perhaps within) the standing wave/antidune stability field (as previously described by Langford & Bracken, 1987; Rust & Gibling, 1990). Additionally, the upstream direction of inclination and internal geometry of some of the low-angle cross-bedding suggests an antidune origin.

The importance of high-energy flows in the formation of channel deposits is also indicated by the common occurrence of massive or chaotically bedded sandstone, particularly near the base of Facies A1 bodies and storeys, and by the poorly sorted and matrix-rich nature of some sands. It is possible that many of the high-stage flows responsible for depositing sand carried a high proportion of sediment in suspension. Abrupt deceleration of such high-concentration flows could have been responsible for the deposition of poorly sorted, matrix-rich and structureless sands.

The overall impression gained from the internal structure of Facies A1 is of sediment deposition from predominantly high-energy, and at times sediment-charged, stream flows. Flow stage and sediment concentration probably fluctuated both within and between flow events, allowing the abundant preservation of high-energy and nonequilibrium bedforms and sedimentary structures.

Facies A2 – abandonment channel fills

Description. Facies A2 is composed of interbedded sandstone of varying grain size and siltstone, and occurs at the top of some Facies A1 units (Table 1). Fining upward is typical, expressed as a continuous decrease in grain size or through fewer, thinner and finer-grained sandstone beds. The base of the facies may be a sharp and flat or undulating contact, or a continuous transition from the underlying sandstone. The upper boundary is generally a sharp contact with an overlying coal seam (Facies B4), although Facies A2 in places passes upward into fine-grained sediments (Facies B2, B3: Fig. 6). Units of Facies A2 are laterally continuous over at least hundreds of metres. Internal bedding surfaces are generally flat, though both low-angle accretion surfaces and channel forms were noted locally. Shallow channel forms were both incised into and filled by Facies A2 sediments.

Sandstones are mainly poorly sorted and micaceous, but in places are quartzose and well sorted, with symmetrical-rippled bed tops. A variety of small-scale sedimentary structures were noted, most abundantly ripple cross-lamination and small-scale trough cross-bedding. These structures are often disrupted by load-casting, rootlet penetration and simple animal bioturbation. Finely divided plant debris is common on bedding planes, and in finer-grained lithologies interlamination structures (flaser, wavy, lenticular, 'pinstripe' bedding) predominate.

Interpretation. The consistent occurrence of Facies A2 above Facies A1 and its fining-upward tendency together suggest formation during the abandonment of river channels. Accordingly, Facies A2 is interpreted as abandonment fill of the low-sinuosity alluvial channels represented by Facies A1. The fining-upward trend, dominance of lower-flow-regime sedimentary structures and bioturbation suggest deposition under low-energy conditions from waning currents and suspension in standing water. In some cases, sand layers were reworked by low-energy wave activity.

The presence of rootlets suggests that some channels were infilled to the point where plants could colonize the substrate. Such horizons are generally uniform grey in colour, indicating

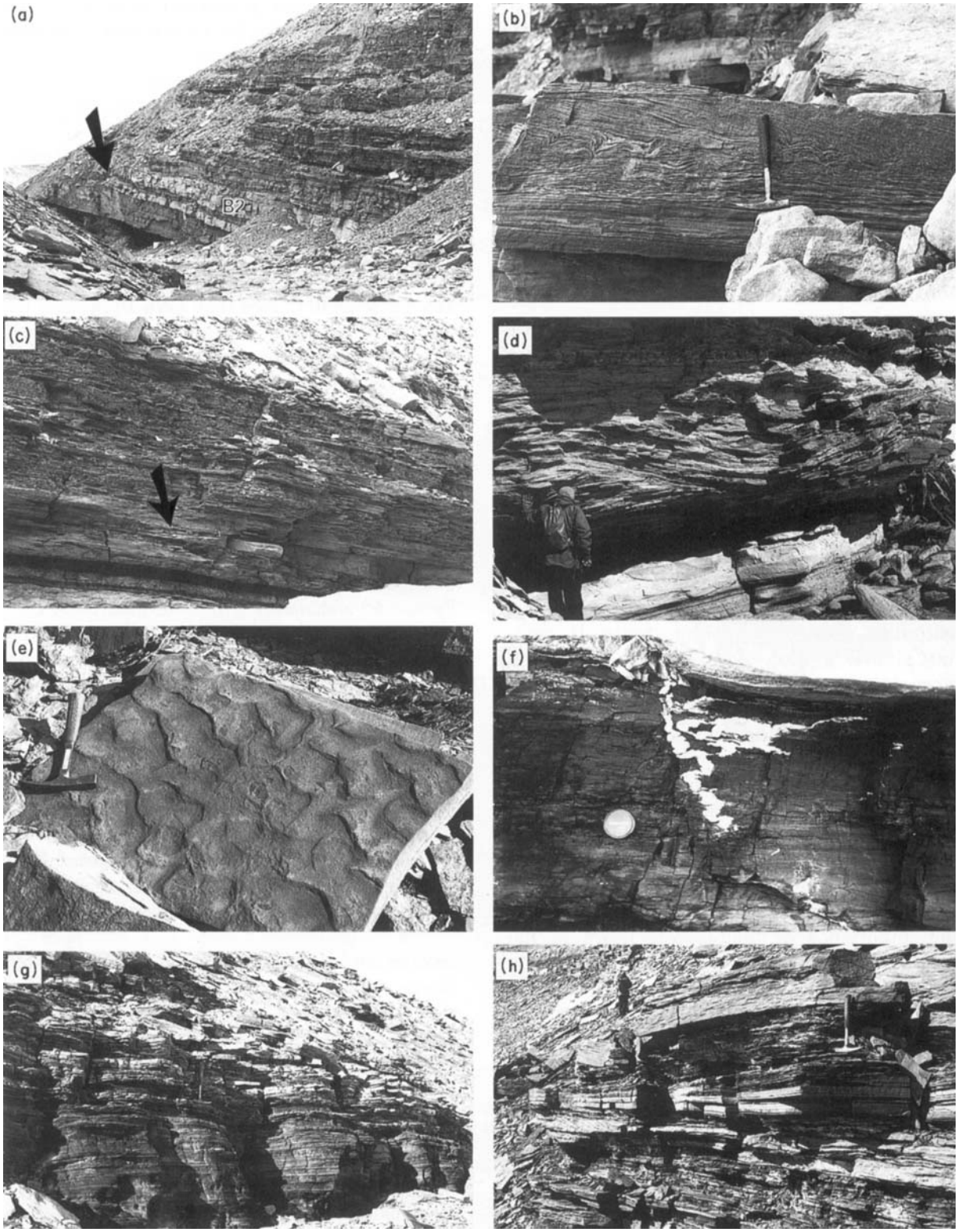
(a)
(b)
(c)
(d)
(e)
(f)
(g)
(h)

permanently hydromorphic conditions, but in places are mottled rust red (5R6/2) or orange-brown (10YR6/6) suggesting partial or intermittent drainage of the alluvial surface (cf. Besly & Fielding, 1989).

The context of Facies A2 suggests that it accumulated during progressive abandonment of alluvial channels, as a precursor to peat formation.

Facies Association B – Floodbasin

Facies B1 – proximal overbank

Description. Facies B1 comprises an association of sharply bounded, tabular sandstone units individually 0·5–1·5 m thick and thinly interbedded sandstone/siltstone (Fig. 10a,b). The vertical arrangement of beds shows no obvious grain-size trend, rather the different lithologies are randomly stacked. Vertical contacts with other facies may be either sharp or gradational, as Facies B1 is typically overlain by other Association B facies (Fig. 6). Facies B1 occurs either in abrupt lateral contact with Facies A1 or passes gradationally into other Association B facies.

Facies B1 units are generally laterally continuous over tens to hundreds of metres. Bedding is mainly flat, but in places shows slight inclination or shallow channel forms. Thick, sharp-bounded beds are continuous over at least 100–200 m, and some beds thin laterally (Fig. 10a). Sandstones typically show flat and low-angle lamination with parting lineation, cross-bedding and ripple cross-lamination (often in climbing forms; Fig. 10b). A variety of soft-sediment deformation structures disrupt the primary fabric of Facies B1, including convolute bedding, flame structures (Fig. 10b), sedimentary dykes and load casts. The basal parts of some beds contain abundant siltstone clasts, whereas others show upright, *in situ* tree stumps, rooted in underlying siltstones. Plant rootlets are common towards the tops of some beds. Thinly interbedded sandstone/siltstone layers contain mainly lenticular and 'pinstripe' bedding, soft-sediment deformation and rare bioturbation structures.

Interpretation. From their relationship to Facies A1/A2 and unconfined, sheet geometry, Facies B1 units were evidently deposited in nonchannel environments. This is further supported by the lack of evidence for pronounced incision, and the wide spread of palaeocurrent directions (Fig. 8). Facies 3 was deposited by a series of initially high-energy, waning current flows, which gave rise to the sharply based sandstone beds, and quieter conditions typified by gentle currents and suspension fallout.

Of all nonchannel facies within the BCM, Facies B1 is the most coarse-grained, and laterally has been noted passing abruptly into major channel sandstones. It may therefore be regarded as representing floodbasin environments proximal to channel margins. The sharply based (locally channellized) sandstones are similar in character to splays described from modern environments (e.g. Farrell, 1987; Smith *et al.*, 1989; Tye & Coleman, 1989; Smith & Perez-Arlucea, 1994) and interpreted from ancient fluvial/fluviolacustrine deposits (e.g. Fielding, 1984; Guion, 1984; Mjos *et al.*, 1993; Jorgensen & Fielding, 1994), particularly the proximal portions of such splays.

Facies B1 is interpreted as representing proximal overbank environments on a broad alluvial plain, where sediment supply was by overbank sheet flow and perhaps also crevassing, during floods. Water depths were sufficiently shallow as to allow establishment of trees on some surfaces.

Fig. 10. Views of Association B and C facies. (a) General view of Glossopteris Gully (Section B) looking north-west, showing the interval 10–60 m on Fig. 6. Note the progressive westward pinchout of the upper of two prominent sandstone bodies (arrowed), and the marked depositional dip displayed by Facies B2 sediments immediately above (labelled B2).(b) Sandstone bed from Facies B1 (Section B), showing cross-bedding, climbing ripples and associated water escape structures. Hammer is 0·25 m long. (c) View of Facies B2–4 in Section B at 90 m on Fig. 6, showing the occurrence of a lensoid sandstone bed (by hammer, 0·25 m long) enclosed by more laterally extensive sandstone and siltstone units, within Facies B2. (d) Section through a small channel incised into, and filled by, Facies B2 (Section H). This feature is interpreted as a splay channel, formed in an overbank environment proximal to the margin of a major alluvial channel. Geologist is 1·9 m. (e) Bedding plane surface in Facies B2 sandstone showing a form set of sinuous-crested current ripples (Section B, hammer 0·28 m long). (f) Coal seam (Facies B4) in Section B, cut by a ptygmatically folded sandstone dyke. The coal is overlain by Facies A1 channel sandstone (interval 60–65 m on Fig. 6). Lens cap is 50 mm in diameter. (g) Claystones with minor very fine sandstone laminae (Facies C1), passing upward into thin-bedded sandstone/siltstone of Facies C2. Dragon's Teeth Member, north side of Bainmedart Cove, hammer is 0·25 m long. (h) Thin-bedded sandstones and siltstones of Facies C2 passing upward into thicker sandstones of Facies C3, Section H (see Fig. 11). Hammer is 0·25 m long.

Although no levee topography could be established during the present study, it is likely that Facies B1 represents the most elevated areas of the alluvial plain. Such elevated settings are commonly the sites of pioneer vegetation growth in waterlogged fluvial environments (see references above).

Facies B2 – overbank

Description. Facies B2 consists predominantly of thinly interbedded siltstone and sandstone in varying proportions, with occasional sharp-bounded sandstone beds up to 1·0 m thick (Fig. 10a,c). Sandstones range from very fine to medium grained, but are mostly fine grained. Both coarsening-upward and fining-upward trends are developed over short intervals, in some instances both within a single unit: such trends are typically manifested by changes in the proportion of interbedded sandstone. Facies B2 passes laterally into Facies A1, and both laterally and vertically into other Association B facies (Fig. 6).

Facies B2 is laterally continuous over distances ranging up to at least several hundred metres. Thicker component beds are also laterally extensive, but in many cases pinch and swell with both basal scouring and top-surface undulation evident (Fig. 10c). Most commonly, internal bedding is flat and form-concordant, but two significant exceptions to this norm have been noted. Some intervals show a persistent depositional dip of 5–10° (e.g. Fig. 10a), with palaeocurrent from sedimentary structures either down or oblique to the depositional dip. Small-scale channel features were also observed in a few places, both incised into and filled by thinly interbedded Facies B2 sediments (Fig. 10d). Both low-relief, undulating features and narrow, relatively steeply incised channels up to 1·5 m deep (e.g. Fig. 10d) were noted.

The thicker sandstone beds noted within Facies B2 are similar in all respects to those of Facies B1. What distinguishes the two facies is the relative dominance of such thick beds in Facies B1, and paucity in Facies B2. Thin sandstone beds in Facies B2 (e.g. Fig. 10c,e) range up to 0·1 m thick and contain small-scale cross-bedding, ripple cross-lamination, climbing ripples and a host of interlamination structures. As in other facies, ripples are straight or sinuous-crested (Fig. 10e). Flat and low-angle lamination is present in places, as is evidence of wave reworking of sands. Small-scale soft-sediment deformation structures occur particularly in thicker sandstone beds. One exposure showed a series of small, listric, normal growth faults with downdip displacements of a few centimetres in the direction of palaeoflow. Sediments on the hangingwall side of these faults contain loop structures (small, detached, recumbent folded sandstone masses), suggestive of small-scale slump movements.

Siltstones are typically medium to dark grey and carbonaceous, in places displaying a fissility. Finely divided (comminuted) plant debris is abundant on bedding planes, and less commonly horizons rich in *Glossopteris* leaves. *In situ* tree stumps up to 15 cm in diameter were noted in a few localities, and strata are pervasively root-penetrated. Simple and branching, tubular, sand-filled burrows (*Planolites, Palaeophycus*) are present in modest numbers in thin-bedded sediments, with rare, straight tracks and trails.

Interpretation. The gross similarities between Facies B1 and B2, and their interfingering lateral relationship, suggest similar processes and environments of deposition. The major difference between the two facies is the lesser proportion of thick, tabular sandstone beds in Facies B2, and concomitant increase in thinly interbedded sandstone/siltstone. This may logically be interpreted as reflecting increased distance from major channel margins from whence coarse sediment was supplied, or alternatively times of decreased sediment supply to the floodbasin.

Facies B2 is interpreted as representing sediment accumulation in more distal and/or less active overbank (floodbasin) settings than Facies B1, where by analogy with studies of modern overbank systems (e.g. Smith *et al.*, 1989) splay deposits are less abundant and thinner than in proximal settings. Some depositional topography is implied by the gentle depositional dips observed at some localities (e.g. Fig. 10a), most likely reflecting a gradient from a proximal levee 'platform' down into shallow standing water of the floodbasin. This surface was evidently prone to incision by some overbank (crevasse-derived or sheetflood) currents which gave rise to the small channels noted. Other sediments were laid down from decelerating currents under shallow water, and at times reworked by gentle wave action.

Facies B3–distal floodbasin

Description. Facies B3 comprises thinly laminated, often carbonaceous siltstones and claystones with minor, thin sandstone laminae. Plant

debris is common on bedding planes, *in situ* rootlets occur in some examples and upright trees were noted in a few cases. Facies B3 occurs in vertical and lateral association with other Association B facies, and intervals are rarely greater than 1 m thick (Fig. 6). Lateral extent is similar to other floodbasin facies.

Interpretation. Facies B3 is interpreted as representing parts of the floodbasin isolated from regular flood incursion and coarse sediment supply, either by distance from active channels or some form of natural barrier. Sediment accumulated mainly by fallout from suspension in stagnant, shallow ponds. Plant debris fell into these ponds and was preserved by the reducing geochemical character of the groundwater. Some occurrences show abundant coalified plant remains, evidently representing a situation transitional from shallow ponds to peat-forming mires (see Facies B4).

Facies B4–mire

Description. This facies comprises seams of black coal and carbonaceous shale up to 4·5 m thick in the study area, but up to 8 m in other parts of the outcrop belt (Fig. 10f). Coal beds thicker than 0·5 m appear to have considerable lateral extent (up to at least several kilometres) and continuity, whereas thin seams are of more variable extent and less persistent, being prone to erosion by channel sandstone bodies. Very few seam splits were noted or could be inferred.

Coals are macroscopically dull and banded (mainly 'Db' according to the Australian Standards scheme) and compositionally layered into 'plies' of 0·1–1·0 m thickness. In hand specimen, most coals display a lustre intermediate between bright and dull end-members, due to small-scale interlayering of coal macerals with varying lustre. Microscopically, this character is reflected in a diverse petrographic assemblage, with modest vitrinite contents and high proportions of 'intermediate' microlithotypes noted by Bennett & Taylor (1972).

The coals typically show inherent ash contents ranging from 15 to 30%, and sulphur 0·5–0·6% (Bennett & Taylor, 1972). Coal seams at outcrop are typically sulphur-stained, giving the false impression of elevated sulphur content. Seams are generally free of clastic partings, with only thicker seams having more than one discrete (claystone or siltstone) parting. Some seams show ptygmatically folded clastic dykes penetrating the seam roof from overlying lithologies (e.g. Fig. 10f).

Interpretation. Facies B4 is interpreted as arising from peat accumulation in wetland environments. Peat formation was evidently *in situ*, from the abundance of plant roots and rootlets immediately beneath coal seams, and was only rarely interrupted by flood-borne sediment incursions. From their petrographic character, coals are inferred to have been derived from a variety of plant materials, including wood of various sizes, leaves, roots and bark, similar to other *Glossopteris*-derived coals (Diessel, 1992). Ash and sulphur levels quoted are typical for alluvial plain coals, which are formed at a distance from the marine sulphate source that affects deltaic and other coastal plain coals, but which are more prone to clastic dilution than their coastal plain counterparts (Fielding, 1985). No evidence was found to support the notion of raised, rainwater-fed (ombrotrophic) mires, rather the sheet geometry of coals at this stage favours a low-lying, rheotrophic mire environment.

Sandstone dykes are common in the BCM coals, but uncommon in a worldwide context. At some localities, clastic dykes in coals were orientated parallel to palaeoflow in an overlying channel sandstone (Facies A1) as established from sedimentary structures, suggesting formation at very shallow depths. Their ptygmatically folded geometry argues against formation by desiccation of peat, indeed no evidence was found to support such an interpretation. They are here interpreted as having been injected into uncompacted peats during high-energy fluvial events that succeeded peat accumulation.

Dragon's Teeth Member

The following three facies, C1 to C3, occur only in the Dragon's Teeth Member (Appendix 1), a distinctive fine-grained unit about 300 m above the base of the BCM. The Dragon's Teeth Member typically consists of two or more thin, coarsening-upward successions, each beginning with Facies C1 and passing upward through Facies C2 into Facies C3 (Fig. 11). The base of the member is marked by an enigmatic horizon of petrified wood and peat, which occurs between a coal seam (Facies B4) and the overlying Dragon's Teeth Member claystones (Facies C1: Fig. 11).

Facies C1 – lake floor

Description. Facies C1 consists of intervals of fissile, carbonaceous claystone (shale) up to

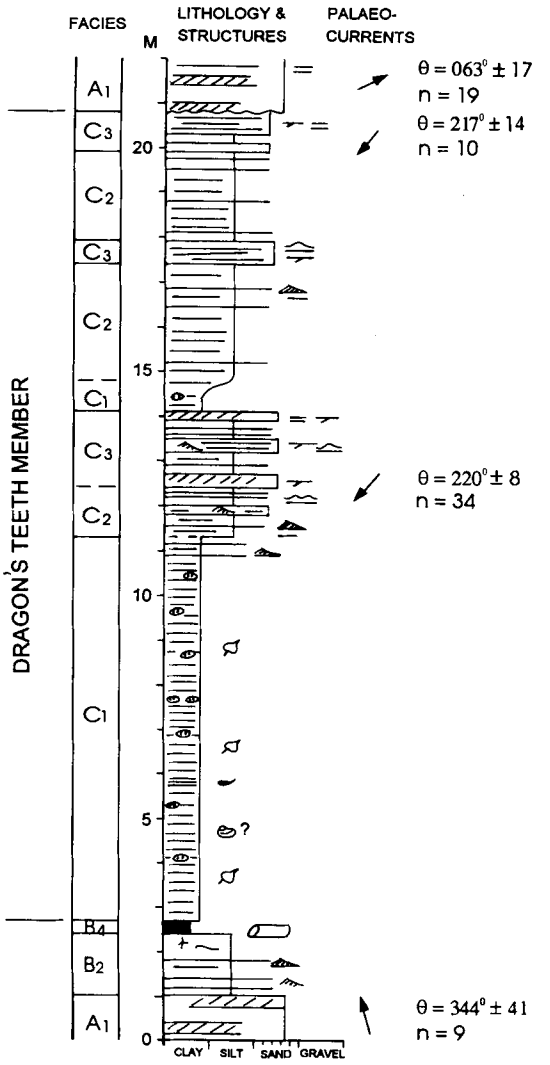

Fig. 11. Graphic log of the Dragon's Teeth Member in Section H. Note the division of the unit into crudely upward-coarsening sequences, and the occurrence of a petrified wood/peat horizon at the base of the unit. See Fig. 6 for key to symbols used.

9 m thick, with horizons containing abundant, rust-coloured concretions (Fig. 10g). These siderite concretions are generally disc-shaped and preserve impressions of *Glossopteris* leaves. Finely divided plant debris is abundant. One questionable bivalve shell was the only animal fossil found in this facies.

Facies C1 invariably occurs at the base of the Dragon's Teeth Member where examined, and at the base of other coarsening-upward sequences within the member. The facies passes gradationally upward into Facies C2, with generally minor interlamination of fine sandstone below the boundary (Fig. 11).

Interpretation. The lithology of Facies C1 suggests deposition from suspension in quiet, standing water. An absence of coarse sediment supply is indicated. A lack of current- or wave-generated sedimentary structures implies low-energy conditions and minimal bottom current activity. The thickness of coarsening-upward sequences combined with the absence of *in situ* vegetation suggests water depths of 5–10 m. Facies C1 is interpreted as quiet-water deposits of a lake or lakes, formed initially by the rapid drowning of the alluvial plain surface (Fig. 11).

Facies C2 – distal lake delta

Description. Facies C2 consists of interlaminated and thinly interbedded siltstone and fine-grained sandstone in intervals up to 5 m thick which coarsen upward (Fig. 10g,h). Siltstones are typically carbonaceous, but do not contain concretions. Sandstones are internally dominated by current-generated interlamination structures (lenticular bedding etc.). Sandstone beds, which are mostly sharp-bounded, range up to 0·05 m thick and are apparently sheet-like. Facies C2 overlies Facies C1 and is in turn overlain by Facies C3 (Fig. 11).

Interpretation. Facies C2 evidently represents the introduction of sand-grade sediment into the quiet lacustrine environment of Facies C1. Sand was carried into the lake via low-energy, tractional currents. Palaeocurrent data suggest sediment derivation from north of the study area (Fig. 8). The vertical sequence character of Facies C2 and C3 is reminiscent of shallow lacustrine deltaic deposits (cf. Farquharson, 1982; Fielding, 1984; Haszeldine, 1984; Tye & Coleman, 1989; Glover & O'Beirne, 1994). In such systems, thinly interbedded sand/silt lithologies are typical of the initial stages of lacustrine delta progradation. Facies C2 is here interpreted as distal lacustrine deltaic deposits, arising from the initial establishment of such deltaic systems.

Facies C3 – proximal lake delta

Description. Facies C3 is again characterized by interbedded sandstone and siltstone, but in this case dominated by mainly medium-grained sandstone beds 0·2–0·4 m thick (Figs 10h and 11). Sandstone beds are laterally extensive and sharp-bounded, and internally show ripple cross-lamination, well-developed climbing ripples, trough cross-bedding and low-angle,

bottomset-dominated cross-bedding similar to that described from Facies A1. Rare, complete antidunal bedforms were observed, with wavelengths of 1·5–2·0 m. The low-angle bedding is intimately associated with the other structures mentioned above, and no wave-formed structures were noted.

Interpretation. The vertical sequence context of Facies C3 together with its lithology argue for an origin in the proximal, shallow-water parts of lacustrine deltaic systems (Fig. 11). Bed geometry and sedimentary structures indicate sediment deposition from decelerating tractional currents, under friction-dominated outflow conditions. Such conditions are typical of small-scale deltas prograding into lakes and other water bodies with gently sloping floors (cf. Tye & Coleman, 1989). The presence of flat lamination and the low-angle cross-bedding described above suggest the existence of critical to supercritical flow conditions at times during the deposition of sediments. Coarse sediment supply to the delta front was episodic, perhaps seasonal, and alternated with periods when finer material settled out of suspension. That this finer sediment was to a considerable extent preserved implies either low-energy depositional conditions at all times (unlikely given the above) or a rapid rate of relative base-level rise during accumulation of the Dragon's Teeth Member.

DEPOSITIONAL SETTING

During the Late Permian, the Prince Charles Mountains area lay at a latitude of around 60°S and probably experienced a humid, cool temperate climate (Powell & Li in Tewari & Veevers, 1993; Webb & Fielding, 1993a). The overall depositional setting envisaged for the BCM is a broad alluvial valley in which braided rivers flowed northward down a tectonically tilted palaeoslope. These deep, at times swiftly flowing rivers deposited large volumes of sand derived from distant sources, constructing channel belt sand bodies of uncertain dimensions. Areas away from active channels were waterlogged floodbasins where overbank and splay sediments accumulated during flood events, and at times of minimal clastic sediment supply extensive wetlands developed where organic-rich sediments accumulated to form peat. An analogous situation (geologically and climatically) exists today in parts of the alluvial valleys of western Canada (Cant & Walker, 1978; Smith *et al.*, 1989) and their Tertiary counterparts (Long, 1981; Smith, 1989).

The BCM are interpreted as having accumulated during a period of northward, axial drainage along a continental rift valley. Coal-bearing alluvial deposits of comparable age are also preserved in other parts of Gondwana, including the Son-Mahanadi and Godavari Valleys of India (Casshyap & Tewari, 1984, 1987), the Bowen and Collie Basins of Australia (Draper & Beeston, 1985; Le Blanc Smith, 1993) and the Transantarctic Mountains (Barrett *et al.*, 1986; Isbell & Collinson, 1991). The BCM also bear broad similarity to Carboniferous coal-bearing successions in maritime Canada (e.g. Hamblin, 1992; Browne & Plint, 1994; Calder, 1994; Plint & Browne, 1994). All of these examples are regarded as having accumulated in elongate, tectonically active basins, and involve comparable temporal and spatial variability in interpreted depositional environments.

The facies assemblage observed within the BCM is similar to other published descriptions of alluvial coal measures (e.g. Long, 1981; Ethridge *et al.*, 1981; Gersib & McCabe, 1981; Flores, 1983; Turner & Whateley, 1983). As previously noted by Fielding (1985), alluvial coal measure successions display a much less varied array of interchannel depositional facies than their delta plain counterparts, in particular lacking the deposits of crevasse-borne minor delta systems that are typical of interdistributary lakes and bays (Tye & Coleman, 1989). Such minor delta deposits are also lacking from the BCM, with the exception of the Dragon's Teeth Member where they dominate the vertical sequence (Fig. 11). Short (1–2 m), coarsening-upward intervals are, however, well preserved and interpreted as distal splays (cf. Smith & Perez-Arlucea, 1994).

The Dragon's Teeth Member (DTM) preserves a record of lacustrine conditions within a discrete part of the coal measure succession. As such, the facies association and its component facies recognized within the DTM are unique to that unit within the Amery Group. A major relative rise in base-level caused flooding of the alluvial plain to form a lake, which after a (possibly considerable) period of time was filled by pulsed supply of coarse sediment from a northerly source (Fig. 8). Ultimately the lake was completely filled and alluvial plain conditions were re-established. The palaeoflow anomaly recorded in the DTM may be explained in terms of the (temporarily) disrupted depositional setting, and is not considered to reflect any change in regional palaeoslope.

Vertical sequence considerations (see below) suggest strongly that major temporal variations in depositional environment occurred within the BCM, in addition to lateral facies variations evident from direct observation of coeval deposits and by application of Walther's Law. In particular, the sheet-like geometry and lack of clastic partings within coal beds imply peat accumulation at times of virtually no clastic sediment supply to the entire area. This theme will be pursued further, following consideration of sediment body architecture.

SEDIMENT BODY ARCHITECTURE

The initial impression gained from field studies of the BCM is of a 'layer-cake' internal stratigraphy. Most of the laterally extensive strike-parallel sections (e.g. Fig. 3), however, are also parallel to palaeoflow and hence to the elongation direction of channel sandstone bodies (Facies A1). A more realistic view of internal stratigraphic heterogeneity may be gained by correlation between equivalent sections perpendicular to palaeoflow (e.g. Fig. 6). From such an exercise, it is evident that sediment bodies, in particular channel sandstones, have limited transverse dimensions. The internal architecture of sediment bodies is considered in more detail below.

Description. Margins of channel sandstone bodies, where exposed, display a wedge geometry indicating up to 4 m of incision and, in a few cases, up to at least 8 m of incision (Fig. 7c). At such margins, Facies A1 either pinches out entirely or passes continuously into thin overbank 'wings' which may extend for at least tens of metres (Fig. 7c). Lateral equivalence with interbedded Association B facies may be established in several cases (Fig. 7a,b). The bases of sandstone bodies are generally flat, in most cases directly overlying coal seams. Rarely was erosional truncation of coal by sandstone bodies observed (but see Fig. 7c).

Internally, Facies A1 bodies are composites of sheets and lenses, mainly composed entirely of sandstone but also including some interbedded sandstone/siltstone (Fig. 7a–c). Sandstone sheets (or 'storeys') are continuous over hundreds of metres parallel to palaeoflow, and tens of metres in a transverse direction. Their boundaries, and internal bedding surfaces, may undulate where soft-sediment deformation features are evident. Lenses are associated mainly with internal channelling within Facies A1 bodies. Small-scale channel features are common, varying from low-aspect-ratio forms (typically 1–2 m × 20 m, with concentric or more complex fill) to symmetrical, concentrically filled channels up to 10 × 40 m (Fig. 7a). The latter style of channel in particular is associated with incision surfaces traceable within sandstone bodies for hundreds of metres, which may cut through significant intervals of previously deposited sediment.

Association B facies are more sheet-like, both in external and internal geometry. Rarely, outcrops showing inclined major bedding planes were noted (Fig. 10a), and some variety in internal form was also noted. In particular, minor channel forms were found in some interpreted floodbasin facies (e.g. Fig. 10d), and some thin sandstone beds were found to be lensoid in flow-transverse section (Fig. 10c). Coals appear to be sheet-like in geometry, and no unequivocal seam splits were identified. However, significant variations in coal bed thickness were noted between sections a few hundred metres apart (Fig. 6).

Interpretation. Many Facies A1 channel bodies are incised into underlying sediments: from this it may be inferred that avulsion of rivers to new sites involved variable levels of excavation of previously deposited alluvium. Incision was not confined to avulsive events, however, and also occurred during the life of individual river courses. Although this was generally on a modest scale, evidence for up to 10 m incision is preserved within Facies A1 bodies. During the excavation of new alluvial channels, erosion was generally limited to the depth of the first significant coal seam encountered in the subsurface. This is a common feature of coal measure sequences worldwide (McCabe, 1984), and is interpreted as arising from the considerable cohesive strength of partly compacted peat.

Coarse sediment accumulated in a variety of mainly low-amplitude bedforms, under highly fluctuating flow conditions. The sheet-like nature of sandstone storeys and variation in palaeocurrent direction between some storeys suggest sediment accumulation via downstream and to a lesser extent across-stream migration of large, low-amplitude bars, superimposed on which were smaller dunes. At times, these bedforms were 'washed out' to form flat- or irregular-surfaced sand sheets during periods and in areas of critical to supercritical flow conditions. The abundance of soft-sediment deformation structures (notably convolute bedding and clastic

dykes) suggests that pore-fluid gradients in the immediate subsurface were inherently unstable. The confinement of such structures to channel sandstone bodies argues for an intrinsic control (perhaps cyclical loading arising from marked seasonal variations in water flux), although an external control such as seismic disturbances cannot be excluded.

Floodbasin facies display the sheet-like architecture typical of overbank facies in other alluvial successions. The mostly two-dimensional nature of exposure precludes detailed analysis of component bed geometry, but some pertinent observations may be made. The presence of narrow, concentrically filled channel forms (e.g. Fig. 10d) and lensoid thin sandstone beds in flow-transverse sections, interpreted as proximal and distal splay deposits, respectively, suggests an elongate splay geometry similar to that documented by Jorgensen & Fielding (1994) from Triassic alluvial coal measures from eastern Queensland.

The apparent lack of coal seam splitting by clastic partings is an unusual feature within the context of alluvial coal measures (cf. Horne *et al.*, 1978; Flores, 1983; Jorgensen & Fielding, 1994), although the ash and sulphur levels are typical. These observations together suggest that large areas of the alluvial plain were protected from major clastic influxes for prolonged periods of time, in order to generate the coal bodies preserved within the BCM.

VERTICAL SEQUENCE ARCHITECTURE

Depositional cyclicity

Description. Deposition of the BCM was strongly cyclical (Figs 4 and 6). The cycles are very similar to those described from Euramerican Carboniferous coal measures as cyclothems (Weller, 1930), although the latter often contain limestone which is completely lacking in the BCM. All BCM cycles have sharp bases; most begin with a thick channel fill sandstone facies (A1) that dominates the cycle. The base of some cycles is marked by a thin conglomerate layer. The channel sandstone is overlain, often gradationally, by a channel abandonment facies (A2) and/or one or more floodbasin facies (B1–3); the latter are less volumetrically significant. In most cases the cycles terminate with a coal bed (B4), which is succeeded abruptly (erosively) by the channel sandstone of the next cycle. Many channel sandstones show direct evidence of incision of up to a few metres into underlying substrates. Some cycles, particularly in Section B (Fig. 6), consist entirely of floodbasin facies (B1–4). All cycles represent a progressive decrease in energy of the system, either gradually or (less commonly) rapidly. In general, a rapidly flowing braided river was replaced by a peat mire.

Even the DTM, which represents lake floor and lacustrine deltaic deposits, displays cyclicity (Fig. 11). In Section H, two coarsening-up cycles are clearly developed: each begins with lacustrine shales (Facies C1), which grade upward into interbedded sandstone and siltstone (C2). The sandstone beds become progressively more abundant upward (C3), until at the top of the cycle there is abrupt return to fine grained shales.

In the 300 m section below the DTM there are 32 cycles, and about the same number in the 300 m of measured section overlying the DTM (Figs 4 and 5). The DTM itself, which is about 19 m thick (Fig. 11), has two (or less likely three) cycles. Thus the average compacted thickness of cycles throughout the BCM is 9–10 m. This suggests that the cause of the cyclicity was constant throughout the sequence.

Despite this consistency of thickness, there is a marked change in the relative proportions of different facies through the measured succession (Fig. 12). The percentage of abandonment and floodbasin facies progressively increases upsection, as does the maximum thickness of coal beds. This is accompanied by a decrease in the thickness of the sandstone units.

Causes

Autocylicity. Cyclicity in coal measures and fluvial and deltaic sequences has usually been ascribed to autocyclic processes or to allocyclic (tectonic or climatic) causes (Riegel, 1991; Calder & Gibling, 1994). In autocyclic mechanisms, there may be an intrinsic limitation to mire growth and peat accumulation (Clymo, 1987), or river beds or delta lobes may aggrade until avulsion/lobe abandonment occurs (Allen, 1965). The river or distributary then follows a topographically lower and more efficient path, which aggrades until avulsion/abandonment occurs again. Autocyclic processes may result in more or less regular sedimentary cycles, but there is no inherent reason why these cycles should display the marked regularity of the BCM cycles. Thus it is unlikely that a semirandom autocyclic process could be the driving force behind the cyclicity of the BCM. In addition, there is evidence that many channel and

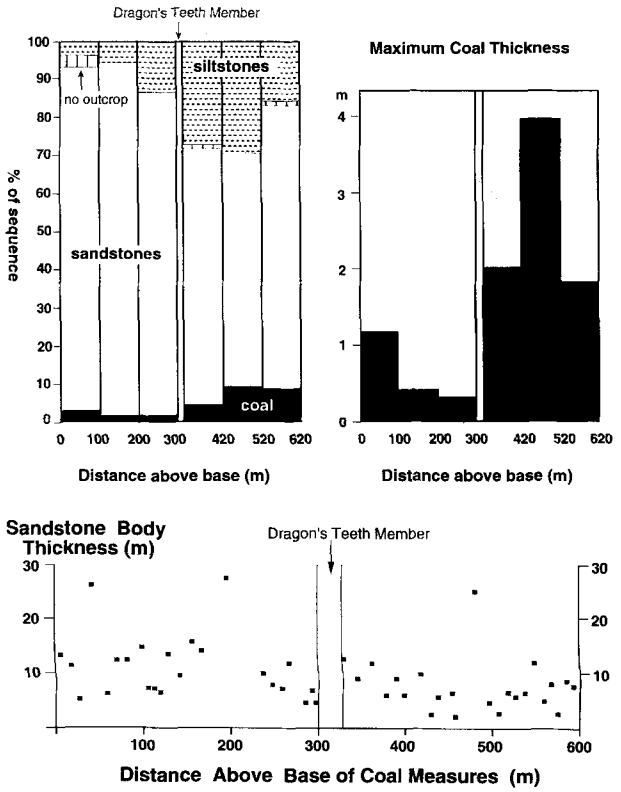

Fig. 12. (a) Plots of lithological variation in 100-m increments through the lower 600 m of the Bainmedart Coal Measures. Note the pronounced changes in sandstone vs. other facies, coal incidence and coal maximum thickness either side of the Dragon's Teeth Member. (b) Plot of Facies A1 sandstone body thickness against height above base of coal measures. Note the gradual up-section decrease in thickness, the scattered occurrence of anomalously thick bodies, and the change across the Dragon's Teeth Member.

delta switching episodes have short periods, e.g. 1000 years (Calder & Gibling, 1994), much less than the average periodicity of the BCM cycles (see below). Interestingly, there is increasing evidence that autocyclicity itself may be climatically driven in some environments; peritidal carbonate cycles, once believed to be autocyclic in origin (e.g. James, 1984), are now generally attributed to climatic fluctuations (e.g. Read *et al.*, 1991), and even deltaic lobe-switching events may have a climatic cause (van Tassell, 1994).

Tectonism. It is self-evident that tectonic processes were active during formation of the BCM, because there must have been subsidence to allow accumulation of 1100 m of coal measures. Tectonic activity could also have been directly responsible for deposition of the DTM. The lacustrine/deltaic facies of this member presumably formed when the river was temporarily dammed to form a large lake. The south-westerly palaeocurrents in the DTM probably reflect the growth of a delta lobe in this direction, rather than a regional reversal of the valley gradient. The lake gradually filled with sediment, following which normal fluvial deposition patterns were re-established. The sudden formation of the lake, and the fact that lacustrine facies occur only once in the entire sequence, suggest that a random event was responsible. The most likely scenario is that uplift occurred along a fault downstream. Similar events have been recorded in river systems throughout the world, although in many cases later downcutting may remove the lacustrine deposits. The Murray River in south-eastern Australia was temporarily dammed about 30 000 years ago by uplift of the downstream side of the Cadell Fault (Brown & Stephenson, 1991).

Further evidence for tectonic activity in the Beaver Lake region is provided by the Radok Conglomerate (which underlies the coal measures; Fielding & Webb, 1995), and the Flagstone Bench Formation, which overlies the BCM (Webb & Fielding, 1993a). Much of the Radok Conglomerate, and the Jetty Member within the Flagstone Bench Formation, record palaeocurrent directions more or less perpendicular to those in the rest of the Amery Group. This is interpreted to represent periodic uplifts of the western flank of the Lambert Graben.

Tectonism could also be responsible for the cyclicity of the BCM. Regular periodic uplifts of the headwater region of the axial drainage system would suddenly increase the energy of the river, resulting in the deposition of coarse-grained facies. As the recently uplifted mountains were eroded and the river gradient concomitantly reduced, lower energy facies would be deposited. Alternatively, subsidence of one side of the graben might divert the river either side of a central range of hills; the abandoned side would then revert to peat mire. Fielding & Webb (1995) suggested that a central uplifted range did exist for at least part of the history of the Lambert Graben.

However, it is extremely unlikely that earth movements could occur with the remarkable regularity demonstrated by the BCM cycles. The cyclicity implies a control not readily explained by random fault adjustments or other tectonic processes (Calder, 1994). Indeed, the uplifts that are apparently recorded within the sequence (DTM and Jetty Member) are random and infrequent.

Climatic (Milankovitch) cyclicity. The Earth's orbit around the sun is influenced by the gravitational attraction of the moon and other planets. This produces long-period fluctuations, called Milankovitch cycles, in the precession of the equinoxes (19- and 23-kyr periodicity), the obliquity of the Earth's axis (41 kyr) and the eccentricity of the orbit (average 100 kyr) (Imbrie & Imbrie, 1979). The values of the periodicities for precession and obliquity have progressively changed with time, because the Earth–Moon distance and day length have been increasing (Berger & Loutre, 1994). In the Late Permian, when the BCM were deposited, the estimated values are 17·5 and 21 kyr for precession, and 35 kyr for the major obliquity cycle.

The orbital fluctuations cause changes in the solar radiation (insolation) reaching the Earth's surface, and in particular in the relative insolation at high and low latitudes. This can cause glaciers to advance and retreat, thereby lowering and raising eustatic sea-level. Shallow-marine sediments, particularly carbonates, commonly record Milankovitch sea-level variations (e.g. Koerschner & Read, 1989), even during 'greenhouse' times when glaciers were apparently at a minimum.

Milankovitch orbital variations also affect the winter/summer insolation differences, and therefore the global atmospheric circulation pattern and the monsoon intensity (Perlmutter & Matthews, 1989; Kutzbach & Otto-Bleisner, 1992). Thus rainfall patterns, wind strengths and directions, and storm frequencies can all vary according to Milankovitch cyclicity (de Boer & Smith, 1994). These climatic changes are reflected in many different sedimentary environments, e.g. Milankovitch variations in lake levels (Anderson, 1984; Olsen, 1986), and sediment supply as turbidites to deep sea fans (Weltje & de Boer, 1993).

In terrestrial environments, sediment transport is dependent on the seasonality of rainfall (Cecil, 1990); this changes the balance between rainfall and evaporation, and will be affected by the orbital variables. Cyclicity in terrestrial deposits has been demonstrated for Cainozoic alluvial fans (de Boer *et al.*, 1991; Nemec & Postma, 1993), and is strongly suggested for some Palaeozoic deltas (van Tassell, 1994) and meandering river deposits (Olsen, 1994).

These considerations are particularly applicable to coal measures, where deposition is strongly controlled by climate. Peat can only accumulate where the water table remains high year round, so waterlogging can inhibit decay of the plant material. At present, this requires nonseasonal rainfall evenly distributed through the year in tropical climates. In higher latitude temperate climates, peat can be preserved through lower rainfall winters, because decreased evaporation accompanying the lower temperatures and winter freezing keeps the water tables high (Lottes & Zeigler, 1994). Thus changes in rainfall seasonality accompanying Milankovitch cyclicity will directly affect peat formation.

In particular, Cecil (1990) proposed that peat beds represent times of nonseasonal rainfall, and siliciclastic interbeds are formed by periods of seasonal precipitation, which restricts vegetation cover in upland areas. As the climate in a peat mire region becomes more seasonal, sediment transport increases until the swamp is overwhelmed. In effect, the ability of the peat-forming ecosystem to cope with environmental change is exceeded (Calder & Gibling, 1994).

Cyclicity has long been recognized in coal measures; the typical cyclothem in Euramerican Carboniferous coal-bearing successions comprises metre-scale coal seams with interbedded siliciclastics and carbonates, totalling 10–40 m in thickness (e.g. Calder, 1994). These are believed to accumulate on time-scales of 10 000–100 000 years, and have been ascribed to orbitally driven glacioeustacy and accompanying climatic shifts (Cecil, 1990; Calder, 1994; Calder & Gibling, 1994: Tandon & Gibling, 1994).

In order to test whether Milankovitch climatic variations were responsible for the cyclicity of the BCM, two independent approaches were used: spectral analysis and estimation of cycle duration.

Spectral analysis applies a Fourier transform to a data set to look for regular periodicities. The technique has been applied with considerable success to find Milankovitch cyclicity in sedimentary sequences from a variety of settings (e.g. lakes – Olsen, 1984; deep-sea pelagic carbonates – Claps & Masetti, 1994). For the present study a fast Fourier transform was used with a Hanning window (Huey, 1990). Data were collected by subdividing the stratigraphic sections into four lithologies/facies: conglomerate, channel sandstone (A1), channel abandonment or floodbasin facies (A2, B1–3), and coal (B4). In this way every cycle could be recorded.

In order to have sufficient cycles to give meaningful results, the stratigraphic sections were grouped into two packages, above and below the DTM. The spectra for both these packages (Fig. 13) have a major peak at 9·4–9·5 cycles/100 m (10·5 m/cycle). This peak is also prominent on the spectrum for the entire BCM, and corresponds

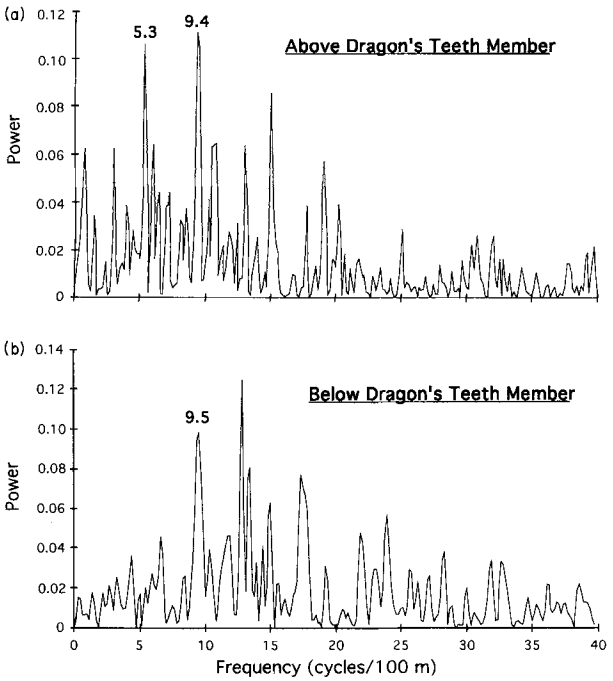

Fig. 13. Spectral series illustrating cyclicity of the BCM (a) below and (b) above the Dragon's Teeth Member. Note the prominent peaks at 5·3 and 9·4 cycles/100 m above the DTM, and at 9·5 below the DTM.

closely to the average cycle thickness (9–10 m). Higher frequency peaks are probably not meaningful, as they disappear on the total spectrum for the BCM. They may be combination tones of the two precessional periods. The spectrum for the package above the DTM has an additional well-defined peak at 5·3 cycles/100 m (19 m/cycle). The ratio of the cycle thickness of the lower frequency peak to that of the higher frequency is 1·8, which is also the ratio of the periodicities of obliquity to precession in the Late Permian (35 and 19 kyr (average), respectively). This suggests that the cycles of the BCM, which form the 9·4–9·5 peaks in the spectra, are due to precessional Milankovitch fluctuations, i.e. each represents about 19 kyr. Superimposed on this cyclicity is a longer period cyclicity, shown by the 5·3 peak, probably due to climatic variations caused by obliquity.

It should be noted that because of the erosive bases of the cycles, it is possible that some amalgamation of cycles may have occurred, such that one measured cycle may in fact represent two or even more. This is not thought to be a serious problem, given the consistency of the cycle thicknesses and facies sequence in each.

To cross-check this line of reasoning, the expected time duration of the BCM was calculated. Total thickness of the formation is about 1100 m. If the cycles average 9–10 m thick throughout the unit, and each cycle represents 19 kyr, then the entire BCM was deposited over 2·1–2·3 Myr. This gives an overall accumulation rate of 480–520 m/Myr. Such rapid subsidence is faster than that experienced by most coal-bearing basins (McCabe, 1991), but similar or even more rapid subsidence has been recorded elsewhere (650–1000 m/Ma in the Carboniferous Cumberland Basin, Nova Scotia; Calder, 1994).

Palynological evidence shows that the Radok Conglomerate, BCM and lower Flagstone Bench Formation (total thickness at least 2·8 km; S. McLoughlin & A. N. Drinnan, unpubl. obs.) all contain Stage 5 microfloras (Playford, 1990). This palynozone effectively spans the entire Late Permian, which represents 10 Myr on almost all time scales (e.g. Harland *et al.*, 1990). The BCM makes up about one-third of the Late Permian sequence in the Lambert Graben, and was therefore deposited over about one-third of the Stage 5 time period or less, i.e. <3·3 Myr, assuming equal depositional rates. This result is in broad agreement with the figure of 2·1–2·3 Myr derived above, and also matches the 1–5 Myr time span of the large-scale sequences (mesothems) within Euramerican Carboniferous coal measures (Calder & Gibling, 1994; Calder, 1994).

If the BCM cycles represented the 100- or 400-kyr eccentricity periodicity, as suggested for some cyclothems elsewhere (e.g. Heckel, 1986; Chesnut, 1989), then the BCM would have been deposited over at least 11 Myr. This time period is unrealistically long, given the calculations above.

Thus it seems likely that the BCM cycles are climatic in origin and each was deposited over about 19 kyr during a precessional fluctuation. It might have been expected that cycles would be due to obliquity periodicity (35 kyr), because at higher latitudes obliquity is generally more prominent (Berger, 1978), and in the Late Permian Antarctica lay virtually at the South Pole. However, different periodicities appear to have been dominant at different times, e.g. 40 kyr in the Pleistocene prior to 700 ka, and 100 kyr after that (Ruddiman *et al.*, 1986).

Depositional mechanisms for the cyclicity

As described above, coal measures may be particularly susceptible to Milankovitch climatic fluctuations, and are likely to record any cyclic changes. In the case of the BCM, seasonality of

rainfall is the simplest explanation for the cyclicity, as suggested by Cecil (1990) for the Euramerican Carboniferous cyclothems. During times when the rainfall was evenly distributed through the year, water tables were consistently high, so widespread peat mires developed, extending several kilometres in both dip and strike directions, and probably occupying almost the entire graben floor. A river system of narrow channels with a low clastic load probably flowed through the swamps. As the climate changed and became more seasonal, the rate of peat accumulation decreased or stagnated, because water tables fell in the drier months. This would have made the peat mires susceptible to burial, as the river changed into a very broad braided system with a high bedload, fed by erosion from the uplands that probably lost vegetation cover as the rainfall became more seasonal. Deposition within the braided channels was characterized by periodic floods that deposited high-energy channel sands with nonequilibrium bedforms.

Support for this scenario comes from considerations of the global circulation changes accompanying Milankovitch cycles (Perlmutter & Matthews, 1989). The subpolar divergence between the Ferrel and Polar Cells shifts during Milankovitch cycles, so that at polar latitudes of 60–70°S (the approximate position of the BCM in the Late Permian), the rainfall changes substantially, from humid to dry, and seasonality will probably differ also.

Silicified *Glossopteris* wood has been recovered from the top of one coal seam in the BCM (Weaver *et al.*, in press); the growth rings are well developed and uniform, suggesting a seasonal climate with limited interseasonal variation. However, given the high latitudes, tree growth was probably controlled by light availability. The growth rings are likely to reflect a slowdown in growth during the extended winter darkness, rather than seasonal variation in rainfall.

It is notable that the bases of BCM cycles are always sharp (apart from those in the DTM). Thick channel sandstones generally directly overlie coal seams, and the basal sandstone bed often incorporates *Glossopteris* tree trunks that presumably grew in the underlying mire. The initiation of each cycle may represent the sudden crossing of a threshold, probably when the river discharge was sufficient that it could break out of its narrow confined channel and flood across the adjacent forested peat mires. Thus the top of each coal seam represents a time line, as proposed for Euramerican Carboniferous cyclothems (Calder & Gibling, 1994). However, there was a gradual build-up to this facies change, as peat accumulation slowed, and discharge and sediment load in the river system progressively increased, to the point where the river had sufficient energy to overwhelm the *Glossopteris* forests, knocking over the trees and almost instantaneously turning the swamp into a braided channel system. The gradual increase in river discharge at the beginning of each cycle is clearly shown by the gradational bases of the coarsening-upwards cycles in the Dragons Teeth Member (Fig. 11). No threshold needed to be crossed for sediment supply to the lake delta to increase, and a progressive progradation of the delta resulted.

Each cycle in the BCM records a complete change in the river system and style of deposition within the entire graben, rather than a gradual abandonment of the river as it avulsed or migrated under steady-state conditions. The changes up-section, e.g. from proximal to distal floodbasin facies (B1 to B2), represent a progressive decrease in the energy of the river as it transformed from a wide braided planform to perhaps a network of narrower channels, rather than the classic explanation of increasing distance from a major channel as it gradually altered course. Similar relationships, on a much more rapid time scale, can be seen in the modern 'Channel Country' rivers of central Australia, which have narrow, anabranching perennial channels, but transform to a broad braidplain during severe floods (Nanson *et al.*, 1988).

This hypothesis readily explains the complete lack of interfingering between channel deposits and the lack of clastic partings and seam splits within coals, all features which are normally characteristic of alluvial coal measures. The channel sandstones and coals are not lateral equivalents. Rather than the fluvial and mire facies existing side by side, as suggested by Walther's Law of Facies, one temporally succeeded the other, in response to episodic, allogenic controls (cf. Anderson & Goodwin, 1990). The different facies represent different periods of sediment accumulation on the graben floor. Nevertheless, refuges of peat mire probably coexisted with the braided river system, perhaps as small pockets along the edge of the graben, so that the mire facies could quickly re-establish when the climate became favourable.

Cyclicity within the DTM, represented by periodic progradation of lacustrine delta lobes, is also readily explained by fluctuations in

sediment supply resulting from Milankovitch-driven variations in rainfall. During periods of more evenly distributed rainfall clays accumulated, owing to the low sediment supply to the river from the vegetated uplands. As rainfall became more seasonal, the increased sediment supply to the river caused a delta lobe to prograde out. Van Tassell (1994) showed that cycles in the Devonian Catskill delta of the eastern USA could be explained by a similar mechanism.

The progressive increases up-section in the relative proportions of overbank lithologies and coal (Fig. 12) may be due to a rise in the subsidence rate, as proposed for other fluvial sequences (e.g. Isbell & Collinson, 1991). When compaction factors are taken into account (2 : 1 for clay to shale; 5 : 1 for well-compacted peat to coal; Ryer & Langer, 1980), the average cycle above the DTM is 4 m thicker than that below the DTM. Since each cycle is believed to represent the same time period (19 kyr), this indicates faster subsidence above the DTM.

CONCLUSIONS

The excellent exposure of the Bainmedart Coal Measures has allowed a detailed facies interpretation, and the very well-developed cyclicity has been interpreted in terms of climatically controlled fluctuations in sediment supply, inferred to result from Milankovitch orbital variations. Calder (1994) came to similar conclusions from a study of a Carboniferous coal-bearing succession in eastern Canada, deposited under humid equatorial conditions. Thus Milankovitch climatic fluctuations can apparently play an important role in fluvial deposition, despite differing ages and palaeolatitudes. Similar cyclicity may be present in any fluvial deposit, although it may be overprinted by local factors or irregularly episodic controls. No study of fluvial sediments should ignore the possible effect of Milankovitch climatic variations.

ACKNOWLEDGMENTS

This work was carried out as part of the Australian National Antarctic Research Expeditions summer programme of 1989/90 in the northern Prince Charles Mountains. The financial and logistical assistance of the Australian Antarctic Division is gratefully acknowledged. In particular, field leader Martin Betts and senior pilot Pip Turner are thanked for their considerable help. Some diagrams were drafted by E. Burdin and T. Bernecker. The constructive reviews of G. Nadon and J. Calder, and editorial advice of G. Plint, are greatly appreciated.

REFERENCES

Allen, J.R.L. (1965) A review of the origin and characteristics of Recent alluvial sediments. *Sedimentology*, **5**, 89–191.

Anderson, E.J. and Goodwin, P.W. (1990) The significance of meter-scale allocycles in the quest for a fundamental stratigraphic unit. *J. geol. Soc.*, **147**, 507–518.

Anderson, R.Y. (1984) Orbital forcing of evaporite sedimentation. In: *Milankovitch and Climate, Part 1* (Ed. by A. L. Berger, J. Imbrie, J. Hays, J. Kukla & B. Saltzman), pp. 147–162. Reidel, Dordrecht.

Baas, J.H., Oost, A.P., Sztano, O., de Boer, P.L. and Postma, G. (1993) Time as an independent variable for current ripples developing towards linguoid equilibrium morphology. *Terra Nova*, **5**, 29–35.

Barrett, P.J., Elliot, D.H. and Lindsay, J.F. (1986) The Beacon Supergroup (Devonian–Triassic) and Ferrar Group (Jurassic) in the Beardmore Glacier area, Antarctica. In: *Geology of the Central Transantarctic Mountains* (Ed. by M. D. Turner and J. F. Splettstoesser), *American Geophysical Union Antarctic Research Series*, **36**, 339–428.

Bennett, A.J.R. and Taylor, O.H. (1972) Coals from the vicinity of the Prince Charles Mountains. In: *Antarctic Geology and Geophysics* (Ed. by R. J. Adie), pp. 591–598. Universitetsforlaget, Oslo.

Berger, A. (1978) Long term variations of caloric insolation resulting from the Earth's orbital elements. *Quat. Res.*, **9**, 139–167.

Berger, A. and Loutre, M.F. (1994) Astronomical forcing through geological time. In: *Orbital Forcing and Cyclic Sequences* (Ed. by P. L. de Boer and D. G. Smith), *Spec. Publ. int. Ass. Sediment.*, **19**, 15–24.

Besly, B.M. and Fielding, C.R. (1989) Palaeosols in Westphalian coal-bearing and red-bed sequences, central and northern England. *Paleogeogr. Paleoclim. Paleoecol.*, **70**, 303–330.

de Boer, P.L., Pragt, J.S.J. and Oost, A.P. (1991) Vertically persistent sedimentary facies boundaries along growth anticlines and climatic control in the thrust-sheet-top south Pyrenean Tremp-Graus foreland basin. *Basin Res.*, **3**, 63–78.

de Boer, P.L. and Smith, D.G. (1994) Orbital forcing and cyclic sequences. In: *Orbital Forcing and Cyclic Sequences* (Ed. by P. L. de Boer and D. G. Smith), *Spec. Publ. int. Ass. Sediment.*, **19**, 1–14.

Bridge, J.S. (1985) Paleochannel patterns inferred from alluvial deposits: a critical evaluation. *J. sedim. Petrol.*, **55**, 579–589.

Brown, C.M. and Stephenson, A.E. (1991) Geology of the Murray Basin, southeastern Australia. *Bur. Miner. Resour. Geol. Geophys. Aust. Bull.*, **235**, 1–430.

Browne, G.H. and Plint, A.G. (1994) Alternating braidplain and lacustrine deposition in a strike-slip setting: the Pennsylvanian Boss Point Formation of the Cumberland Basin, maritime Canada. *J. sedim. Res.* **B64**, 40–59.

Calder, J.H. (1994) The impact of climate change, tectonism and hydrology on the formation of Carboniferous tropical intermontane mires: the Springhill coalfield, Cumberland Basin, Nova Scotia. *Paleogeogr. Paleoclim. Paleoecol.*, **106**, 323–351.

Calder, J.H. and Gibling, M.R. (1994) The Euramerican Coal Province: controls on Late Palaeozoic peat accumulation. *Paleogeogr. Paleoclim. Paleoecol.*, **106**, 1–21.

Cant, D.J. and Walker, R.G. (1978) Fluvial processes and facies sequences in the sandy braided South Saskatchewan River, Canada. *Sedimentology*, **25**, 625–648.

Casshyap, S.M. and Tewari, R.C. (1984) Fluvial models of the Lower Permian coal measures of Son-Mahanadi and Koel-Damodar basins, India. In: *Sedimentology of Coal and Coal-Bearing Sequences* (Ed. by R. A. Rahmani and R. M. Flores), *Spec. Publ. int. Ass. Sediment.*, **7**, 121–147.

Casshyap, S.M. and Tewari, R.C. (1987) Depositional model and tectonic evolution of Gondwana basins. *The Palaeobotanist*, **36**, 59–66.

Cecil, C.B. (1990) Paleoclimate controls on stratigraphic repetition of chemical and siliciclastic rocks. *Geology*, **18**, 533–536.

Chesnut, D.R. (1989) Pennsylvanian rocks of the eastern Kentucky coalfield. In: *Carboniferous Geology of the Eastern United States* (Ed. by C. B. Cecil and C. F. Eble), 28th International Geological Conference Guidebook T143, pp. 57–60. American Geophysical Union, Washington.

Claps, M. and Misetti, D. (1994) Milankovitch periodicities in Cretaceous deep-sea sequences from the Southern Alps (Northern Italy). In: *Orbital Forcing* and *Cyclic Sequences* (Ed. by P. L. de Boer and D. G. Smith), *Spec. Publ. int. Ass. Sediment.*, **19**, 99–108.

Clymo, R.S. (1987) Rainwater-fed peat as a precursor to coal. In: *Coal* and *Coal-bearing Strata* (Ed. by A. C. Scott), *Spec. Publ. geol. Soc. Lond.* **32**, 17–23.

Collinson, J.D. and Thompson, D.B. (1989) *Sedimentary Structures*, 2nd edn. Unwin Hyman, London.

Crohn, P.W. (1959) A contribution to the geology and glaciology of the western part of Australian Antarctic Territory. *Bull. Bur. Miner. Resour. Geol. Geophys. Aust.*, **52**.

Diessel, C.F.K. (1992) *Coal-Bearing Depositional Systems*. Springer-Verlag, Berlin.

Draper, J.J. and Beeston, J.W. (1985) Depositional aspects of the Reid's Dome Beds. *Queensland Governm. Mining J.*, **86**, 200–210.

Ethridge, F.G., Jackson, T.J. and Youngberg, A.D. (1981) Floodbasin sequence of a fine-grained meander-belt subsystem: the coal-bearing Lower Wasatch and Upper Fort Union Formations, southern Powder River Basin, Wyoming. In: *Recent* and *Ancient Non-Marine Depositional Environments: Models for Exploration* (Ed. by F. G. Ethridge and R. M. Flores), *Spec. Publ. Soc. econ. Paleont. Miner.*, **31**, 191–209.

Farquharson, G.W. (1982) Lacustrine deltas in a Mesozoic alluvial sequence from Camp Hill, Antarctica. *Sedimentology*, **29**, 717–725.

Farrell, K.M. (1987) Sedimentology and facies architecture of overbank deposits of the Mississippi River, False River Region, Louisiana. In: *Recent Developments in Fluvial Sedimentology* (Ed. by F. G. Ethridge, R. M. Flores and M. D. Harvey), *Spec. Publ. Soc. econ. Paleont. Miner.*, **39**, 111–120.

Fedorov, L.V., Grikurov, G.E., Kurinin, R.G. and Masolov, V.N. (1982) Crustal structure of the Lambert Glacier area from geophysical data. In: *Antarctic Geoscience* (Ed. by C. Craddock), pp. 931–936. University of Wisconsin, Madison, in press.

Fielding, C.R. (1984) Upper delta plain lacustrine and fluviolacustrine facies from the Westphalian of the Durham coalfield, NE England. *Sedimentology*, **31**, 547–567.

Fielding, C.R. (1985) Coal depositional models and the distinction between alluvial and delta plain environments. *Sediment. Geol.*, **42**, 41–48.

Fielding, C.R. and Webb, J.A. (1995) Sedimentology of the Permian Radok Conglomerate in the Beaver Lake area of MacRobertson Land, East Antarctica. *Geological Magazine*, **132**, 51–63.

Flores, R.M. (1983) Basin facies analysis of coal-rich Tertiary fluvial deposits, northern Powder River Basin, Montana and Wyoming. In: *Modern and Ancient Fluvial Systems* (Ed. by J. D. Collinson and J. Lewin), *Spec. Publ. int. Ass. Sediment.*, **6**, 501–515.

Folk, R.L., Andrews, P.B. and Lewis, D.W. (1970) Detrital sedimentary rock classification and nomenclature for use in New Zealand. *New NZ J. Geol. Geophys.*, **13**, 947–968.

Gersib, G.A. and McCabe, P.J. (1981) Continental coal-bearing sediments of the Port Hood Formation (Carboniferous), Cape Linzee, Nova Scotia, Canada. In: *Recent and Ancient Non-Marine Depositional Environments: Models for Exploration* (Ed. by F. G. Ethridge and R. M. Flores), *Spec. Publ. Soc. econ. Paleont. Miner.*, **31**, 95–108.

Glover, B.W. and O'Beirne, A.M. (1994) Anatomy, hydrodynamics and depositional setting of a Westphalian C lacustrine delta complex, West Midlands, England. *Sedimentology*, **41**, 115–132.

Guion, P.D. (1984) Crevasse splay deposits and roof-rock quality in the Threequarters Seam (Carboniferous) in the East Midlands Coalfield, UK. In: *Sedimentology of Coal and Coal-Bearing Sequences* (Ed. by R. A. Rahmani and R. M. Flores), *Spec. Publ. int. Ass. Sediment.*, **7**, 291–308.

Hamblin, A.P. (1992) Half-graben lacustrine sedimentary rocks of the lower Carboniferous Strathlorne Formation, Horton Group, Cape Breton Island, Nova Scotia, Canada. *Sedimentology*, **39**, 263–284.

Harland, W.B., Armstrong, R.L., Cox, A.V., Craig, L.E., Smith, A.G. and Smith, D.G. (1990) *A Geological Time Scale 1989*. Cambridge University Press, Cambridge.

Harms, J.C., Southard, J.B., Spearing, D.R. and Walker, R.G. (1975) *Depositional Environments as Interpreted from Primary Sedimentary Structures and Stratification Sequences*. Society of Economic Paleontologists and Mineralogists Short Course Notes, 2. SEPM Tulsa.

Haszeldine, R.S. (1983) Descending tabular cross-bed sets and bounding surfaces from a fluvial channel in the Upper Carboniferous coalfield of north-east England. In: *Modern* and *Ancient Fluvial Systems* (Ed. by J. D. Collinson and J. Lewin), *Spec. Publ. int. Ass. Sediment.*, **6**, 449–456.

Haszeldine, R.S. (1984) Muddy deltas in freshwater lakes, and tectonism in the Upper Carboniferous Coalfield of NE England. *Sedimentology,* **31,** 811–822.

Heckel, P.H. (1986) Sea-level curve for Pennsylvanian eustatic marine transgressive-regressive depositional cycles along midcontinent outcrop belt, North America. *Geology,* **14,** 330–334.

Horne, J.C., Ferm, J.C., Caruccio, F.T. and Baganz, B.P. (1978) Depositional models in coal exploration and mine planning in the Appalachian region. *Bull. Am. Ass. petrol. Geol.,* **62,** 2379–2411.

Huey, L.J. (1990) Spectrum instructions. *Notes accompanying Spectrum programme.*

Imbrie, J. and Imbrie, K.P. (1979) *Ice Ages: Solving the Mystery*. Enslow Publishers, Short Hills, NJ.

Isbell, J.L. and Collinson, J.W. (1991) Sedimentological significance of fluvial cycles in the Permian of the Central Transantarctic Mountains, Antarctica. In: *Gondwana Seven Proceedings* (Ed. by H. Ulbrich and A. C. Rocha Campos), pp. 189–199. Instituto de Geociencias-USP, Sao Paulo.

James, N.P. (1984) Shallowing upwards sequences in carbonates. In: *Facies Models,* 2nd edn (Ed. by R. G. Walker), pp. 213–228. Geoscience Canada, Toronto.

Jorgensen, P.J. and Fielding, C.R. (1994) Application of facies and architectural analysis to opencut coal mining: the Late Triassic Callide Coal Measures, east-central Queensland. In: *Proceedings of the 28th Symposium on Advances in the Study of the Sydney Basin*, pp. 228–235. University of Newcastle, Newcastle, NSW.

Kemp, E.M. (1973) Permian flora from the Beaver Lake area, Prince Charles Mountains, Antarctica. I. Palynological examination of samples. *Bureau of Mineral Resources, Geology & Geophysics, Australia, Bulletin*, **126,** 7–12.

Koerschner, W.F. and Read, J.F. (1989) Field and modelling studies of Cambrian carbonate cycles, Virginia Appalachians. *J. sedim. Petrol.,* **59,** 654–687.

Kutzbach, J.E. and Otto-Bleisner, B.L. (1982) The sensitivity of the African-Asian monsoonal climate to orbital parameter changes for 9000 years BP in a low resolution general circulation model. *J. atmos. Sci.,* **39,** 1177–1188.

Langford, R. and Bracken, B. (1987) Medano Creek, Colorado, a model for upper-flow-regime fluvial deposition. *J. sedim. Petrol.,* **57,** 863–870.

Le Blanc Smith, G. (1993) *Geology and Permian coal resources of the Collie Basin, Western Australia*. Geological Survey of Western Australia Report 38.

Long, D.G.F. (1981) Dextral strike-slip faults in the Canadian Cordillera and depositional environments of related fresh-water, intermontane coal basins. In: *Sedimentation* and *Tectonics in Alluvial Basins* (Ed. by A. D. Miall), *Spec. Pap. geol. Soc. Canada*, **23**, 153–186.

Lottes, A.M. and Zeigler, A.M. (1994) World peat occurrence and the seasonality of climate and vegetation. *Paleogeogr. Paleoclim. Paleoecol.,* **106,** 23–37.

McCabe, P.J. (1984) Depositional environments of coal and coal-bearing strata. In: *Sedimentology of Coal and Coal-Bearing Sequences* (Ed. by R. A. Rahmani and R. M. Flores), *Spec. Publ. int. Ass. Sediment.*, **7,** 13–42.

McCabe, P.J. (1991) Tectonic controls on coal accumulation. *Bull. Soc. Geol. Francaise,* **162,** 277–282.

McKelvey, B.C. and Stephenson, N.C.N. (1990) A geological reconnaissance of the Radok Lake area, Amery Oasis, Prince Charles Mountains. *Antarctic Science,* **2,** 53–66.

Mjos, R., Walderhaug, O. and Prestholm, E. (1993) Crevasse splay sandstone geometries in the Middle Jurassic Ravenscar Group of Yorkshire, UK. In: *Alluvial Sedimentation* (Ed. by M. Marzo and C. Puigdefabregas), *Spec. Publ. int. Ass. Sediment.*, **17**, 167–184.

Mond, A. (1972) Permian sediments of the Beaver Lake area, Prince Charles Mountains. In: *Antarctic Geology and Geophysics* (Ed. by R. J. Adie), pp. 585–589. Universitetsforlaget, Oslo.

Nanson, G.C., Young, R.W., Price, D.M. and Rust, B.R. (1988) Stratigraphy, sedimentology and Late Quaternary chronology of the Channel Country of western Queensland. In: *Fluvial Geomorphology of Australia* (Ed. by R. F. Warner), pp. 151–175. Academic Press, Sydney.

Nemec, W. and Postma, G. (1993) Quaternary alluvial fans in southwestern Crete: sedimentation processes and geomorphic evolution. In: *Alluvial Sedimentation* (Ed. by M. Marzo and C. Puigdefabregas), *Spec. Publ. int. Ass. Sediment.*, **17**, 235–276.

Olsen, P.E. (1984) Periodicity of lake level cycles in the Late Triassic Lockatong Formation of the Newark Basin (Newark Supergroup, New Jersey and Pennsylvania). In: *Milankovitch* and *Climate* (Ed. by A. L. Berger, J. Imbrie, J. Hays, G. Kukla and B. Saltzman), Vol. 1, pp. 29–146. Reidel Publishing Co., Dordrecht.

Olsen, P.E. (1986) A 40 million year lake record of Early Mesozoic orbital climate forcing. *Science,* **234,** 842–848.

Olsen, H. (1994) Orbital forcing on continental depositional systems–lacustrine and fluvial cyclicity in the Devonian of East Greenland. In: *Orbital Forcing* and *Cyclic Sequences* (Ed. by P. L. de Boer and D. G. Smith), *Spec. Publ. int. Ass. Sediment.*, **19**, 429–438.

Perlmutter, M.A. and Matthews, M.D. (1989) Global cyclostratigraphy–a model. In: *Quantitative Dynamic Stratigraphy* (Ed. by T. A. Cross), pp. 233–260. Prentice Hall, Englewood Cliffs.

Playford, G. (1990) Proterozoic and Palaeozoic palynology of Antarctica: a review. In: *Antarctic Paleobiology–its Role in the Reconstruction of Gondwana* (Ed. by T. N. Taylor and E. L. Taylor), pp. 50–70. Springer-Verlag, New York.

Plint, A.G. and Browne, G.H. (1994) Tectonic event stratigraphy in a fluvio-lacustrine, strike-slip setting: the Boss Point Formation (Westphalian A), Cumberland Basin, maritime Canada. *J. sedim. Res.*, **B64**, 341–364.

Ravich, G.M., Gor, Yo., G., Dibner, A.F. and Dobanova, O.V. (1977) Stratigrafiya verkhnepaleozoiskikh uglenocnykh otlozheniy vostochnoy Antarktidy (rayon ozera Biver). *Antarktika*, **16**, 62–75.

Read, J.F., Osleger, D.A. and Elrick, M.E. (1991) Two-dimensional modelling of carbonate ramp sequences and component cycles. In: *Sedimentary Modelling: Computer Simulations and Methods for Improved Parameter Definition* (Ed. by E. K. Franseen, W. L. Watney and C. G. St. C. Kendall), *Bull. Kansas Geol. Surv.*, **233**, 473–488.

Reinfelds, I. and Nanson, G. (1993) Formation of braided river floodplains, Waimakariri River, New Zealand. *Sedimentology*, **40**, 1113–1127.

Riegel, W. (1991) Coal cyclothems and some models for their origin. In: *Cycles* and *Events in Stratigraphy* (Ed. by G. Einsele, W. Ricken and A. Seilacher), pp. 733–750. Springer-Verlag, Berlin.

Roe, S.-L. (1987) Cross-strata and bedforms of probable transitional dune to upper-stage plane-bed origin from a Late Precambrian fluvial sandstone, northern Norway. *Sedimentology*, **34**, 89–101.

Roe, S.-L. and Hermansen, M. (1993) Processes and products of large, Late Precambrian sandy rivers in northern Norway. In: *Alluvial Sedimentation* (Ed. by M. Marzo and C. Puigdefabregas), *Spec. Publ. int. Ass. Sediment.*, **17**, 151–166.

Ruddiman, W.F., Raymo, M. and McIntyre, A. (1986) Matuyama, 41,000 year cycles: North Atlantic Ocean and northern hemisphere ice sheets. *Earth planet. Sci. Lett.*, **80**, 117–129.

Rust, B.R. and Gibling, M.R. (1990) Three-dimensional antidunes as HCS mimics in a fluvial sandstone: the Pennsylvanian South Bar Formation near Sydney, Nova Scotia. *J. sedim. Petrol.*, **60**, 540–548.

Ryer, T.A. and Langer, A.W. (1980) Thickness change involved in the peat-to-coal transition for a bituminous soal of Cretaceous age in central Utah. *J. sedim. Petrol.*, **50**, 987–992.

Saunderson, H.C. and Lockett, F.P.J. (1983) Flume experiments on bedforms and structures at the dune-plane bed transition. In: *Modern* and *Ancient Fluvial Systems* (Ed. by J. D. Collinson and J. Lewin), *Spec. Publ. int. Ass. Sediment.*, **6**, 49–58.

Smith, G.G. (1989) *Coal Resources of Canada.* Geological Survey of Canada Paper 89-4.

Smith, N.D. and Perez-Arlucea, M. (1994) Fine-grained splay deposition in the avulsion belt of the lower Saskatchewan River, Canada. *J. sedim. Res.*, **B64**, 159–168.

Smith, N.D., Cross, T.A., Dufficy, J.P. and Clough, S.R. (1989) Anatomy of an avulsion. *Sedimentology*, **36**, 1–23.

Tandon, S.K. and Gibling, M.R. (1994) Calcrete and coal in Late Carboniferous cyclothems of Nova Scotia, Canada: climate and sea-level changes linked. *Geology*, **22**, 755–758.

van Tassell, J. (1994) Cyclic deposition of the Devonian Catskill Delta, of the Appalachians, USA. In: *Orbital Forcing* and *Cyclic Sequences* (Ed. by P. L. de Boer and D. G. Smith), *Spec. Publ. int. Ass. Sediment.*, **19**, 395–411.

Tewari, R. and Veevers, J.J. (1993) Gondwana basins of India occupy the middle of a 7500 km sector of radial valleys and lobes in central-eastern Gondwanaland. In: *Gondwana Eight: Assembly, Evolution* and *Dispersal* (Ed. by R. H. Findlay, R. Unrug, M. R. Banks and J. J. Veevers), pp. 507–512. A.A. Balkema, Rotterdam.

Turner, B.R. and Whateley, M.K.G. (1983) Structural and sedimentological controls of coal deposition in the Nongoma Graben, northern Zululand, South Africa. In: *Modern* and *Ancient Fluvial Sytems* (Ed. by J. D. Collinson and J. Lewin), *Spec. Publ. int. Ass. Sediment.*, **6**, 457–471.

Tye, R.S. and Coleman, J.M. (1989) Depositional processes and stratigraphy of fluvially dominated lacustrine deltas: Mississippi delta plain. *J. sedim. Petrol.*, **59**, 973–996.

Weaver, L., McLoughlin, S. and Drinnan, A.N., in press. Fossil woods from the Upper Permian Bainmedart Coal Measures, northern Prince Charles Mountains, East Antarctica. *AGSO J. Austr. Geol. Geophys.*

Webb, J.A. and Fielding, C.R. (1993a) Permo-Triassic sedimentation within the Lambert Graben, northern Prince Charles Mountains, East Antarctica. In: *Gondwana Eight: Assembly, Evolution and Dispersal* (Ed. by R. H. Findlay, R. Unrug, M. R. Banks and J. J. Veevers), pp. 357–369. A.A. Balkema, Rotterdam.

Webb, J.A. and Fielding, C.R. (1993b) Revised stratigraphical nomenclature for the Permo-Triassic Flagstone Bench Formation, northern Prince Charles Mountains, East Antarctica. *Antarctic Science*, **5**, 409–410.

Weller, J.M. (1930) Cyclical sedimentation of the Pennsylvanian period and its significance. *J. Geol.*, **38**, 97–135.

Weltje, G.-j. and de Boer, P.L. (1993) Astronomically induced palaeoclimate oscillations reflected in Pliocene turbidite deposits on Corfu (Greece): implications for the interpretation of high order cyclicity in ancient turbidite systems. *Geology*, **21**, 307–310.

White, M.E. (1973) Permian flora from the Beaver Lake area, Prince Charles Mountains, Antarctica. 2. Plant fossils. *Bull. Bur. Miner. Resour. Geol. Geophys. Australia*, **126**, 13–18.

Manuscript received 5 January 1995; revision accepted 6 September 1995

APPENDIX 1

Dragon's Teeth Member (new name)

Derivation of name: from the 'Dragon's Teeth', the name given to the cliffs along the north-western side of Radok Lake (Fig. 1).

Distribution: exposure presently confined to cliffs on the northern and southern sides of Bainmedart Cove, and the plateau extending northwards; may extend further north, but covered by moraine (Fig. 1).

Thickness: maximum 18 m; thins to less than 1 m in places.

Boundaries: upper and lower both conformable.

Stratigraphic relationships: base of Dragon's Teeth Member lies 300 m above base of Bainmedart Coal Measures; overlain by at least 800 m of Bainmedart Coal Measures (only lower 300 m measured, remainder estimated from outcrop width and dip of strata).

Lithologies (Fig. 11): interbedded fine- to medium-grained, yellow-brown, thin-bedded sandstones, grey siltstones and dark grey claystones; claystones contain sideritic concretions with well-preserved impressions of *Glossopteris* leaves; sandstones are mostly subarkoses, often cemented by ferroan calcite; sandstones often occur in thickening- and coarsening-upward sequences; thicker beds often contain low-angle or undulatory lamination. Directly beneath Dragon's Teeth Member is a lensoidal unit, usually less than 1 m thick, of silicified wood and peat; apparently representing silicified upper portion of coal seam directly underlying the Dragon's Teeth Member.

Age: mid- to Late Permian; overlying and underlying strata contain Stage 5 microflora (Kemp, 1973; Playford, 1990).

Environment of deposition: lacustrine; the coarsening/thickening-upward sandstone sequences probably represent progradation of small deltas formed where streams entered the lake.